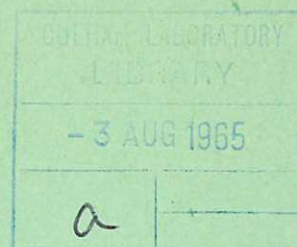


CULHAM LIBRARY
REFERENCE ONLY



United Kingdom Atomic Energy Authority

RESEARCH GROUP

Translation

PULSED PLASMA GUNS
and
INTERACTION BETWEEN PLASMA
BLOBS AND MAGNETIC FIELDS

V. S. KOMELKOV
B. G. SAFRONOV

Culham Laboratory,
Culham, Abingdon, Berkshire

1965

Available from H. M. Stationery Office

FIVE SHILLINGS AND SIXPENCE NET

© - UNITED KINGDOM ATOMIC ENERGY AUTHORITY - 1965
Enquiries about copyright and reproduction should be addressed to the
Librarian, Culham Laboratory, Culham, Abingdon, Berkshire, England.

PULSED PLASMA GUNS

INTERACTION BETWEEN PLASMA BLOBS AND MAGNETIC FIELDS

by

V.S. KOMELKOV
B.G. SAFRONOV

from

Report IAE - 663
I.V. Kurchatov Institute of Nuclear Energy,
Moscow, 1964, pp.1 - 60

Translation prepared by
CULHAM LABORATORY TRANSLATIONS OFFICE

U.K.A.E.A. Research Group,
Culham Laboratory,
Nr Abingdon,
Berks
November, 1964 (C/18 IMG)

C O N T E N T S

	<u>Page</u>
INTRODUCTION	1
<u>P A R T I</u>	
1. COAXIAL GUNS	1
2. COAXIAL GUN WITH PLASMA FOCUSING	9
3. BOSTICK TYPE GUNS	13
4. TITANIUM PLASMA SOURCE	20
<u>P A R T II</u>	
1. MOTION OF PLASMA BLOBS IN LONGITUDINAL MAGNETIC FIELDS	23
2. SEPARATION OF IMPURITIES BY A RAPIDLY INCREASING LONGITUDINAL MAGNETIC FIELD	28
3. INTERACTION OF PLASMA BLOBS WITH A TRANSVERSE MAGNETIC FIELD	30
CONCLUSIONS	38
REFERENCES	40

INTRODUCTION

A brief survey is given of unpublished investigations of plasma guns, and of the interaction between plasma blobs and magnetic fields, carried out lately in the Soviet Union.

The authors did not deem it their duty to give an analysis of the general state of the art, which would be impossible without including a large number of published papers with which plasma physicists specialising in this field are inevitably familiar.

The development of plasma guns has passed the stage where the complexity of the phenomena occurring during the acceleration of the plasma in various systems was not sufficiently appreciated. Work on plasma blobs or guns is carried out at present by a variety of recent continually improved methods, the description of which would form the subject of a separate paper. Whereas until fairly recently the investigators concentrated mainly on data about the gross characteristics of plasma guns, at this stage the study of the micromechanisms determining the main processes taking place in, and the properties of, plasma blobs is becoming increasingly pressing.

P A R T 1

PULSED PLASMA GUNS

1. COAXIAL GUNS

The acceleration of a plasma in systems with coaxial cylindrical electrodes, proposed as far back as 1957⁽¹⁾, was widely adopted following the introduction of electrodynamic valves for pulsed gas admission. Marshall's plasma gun⁽²⁾ which is based on this principle, is used as an injection device in numerous thermonuclear and other experiments.

The quest for the optimum conditions in which the capacitors supply the maximum energy to the accelerated blob, based on the snowplough model and on the general equations of motion with consideration of a variable system inductance, lead to an improved application of the part played in the acceleration processes by the external circuit parameters (R,L,C) and the electrode dimensions. In particular, it was found that maximum efficiency and blob velocity can be expected in conditions where the dimensionless parameter

$$q = \frac{B^2 C^2 V_0^2}{2m L_0} \geq 10 - 100$$

where

- B - is the inductance per unit length of the gun (H/cm)
- C - the capacitance of the bank, (μ F)
- L_0 - the initial circuit inductance (H)
- V_0 - the bank voltage (volts)
- m - the mass of gas accelerated (kg)

However, in actual conditions one has no ideal plasma piston on which to base these calculations. Instead of a continuous plasma surface separate channels are formed in the region of both low and high initial gas densities; in addition to this gas density, the number of these channels is also determined by the external circuit parameters^{(3)*}. These channels have all the properties of spark channels. At the instant of their formation shock waves are observed propagating in the surrounding cold gas. The number of channels depends on the gas pressure in the discharge chamber. When this pressure attains a certain value the total current flows in a single channel. The so-called spatial structures are therefore related to the current-voltage characteristics of the channels, to breakdown processes in the gas at different pressures, and to the conditions of formation of the skin layer. Only under certain defined conditions is a continuous current distribution in the driving layer observed. For a considerable number of accelerating cycles only a fraction of the gas is picked up (accelerated) on the one hand, whilst on the other an intense release of impurities takes place from the electrodes due to high local current densities.

The mass of gas accelerated depends not only on the quantity of gas injected but also on the other parameters of the gun.

Nor does all the current flow in the skin layer^(4,5). It is in fact distributed over the total discharge volume and is ejected from the gun together with the plasma, forming closed eddies^(6,7).

Attempts have been made of late at analysing the complex mechanism of blob generation. Thus, Baranov and Musin, in the general equations of motion, considered the particle diffusion to the electrodes, electrode erosion, etc.⁽⁸⁾ It was shown that in the case of weak erosion the mass of the plasma blob decreases monotonically due to diffusion of the neutral particles. In the case of strong erosion the mass of the blob may considerably exceed that of the gas admitted into the accelerator.

The maximum velocity of the blob corresponds to equality of the electrodynamic forces and the frictional forces acting on the blob. The velocity increases as the electrode erosion increases and as the mass of the gas decreases by diffusion. These conclusions are broadly confirmed by the experimental observations.

The chief experimental information about the operation of coaxial guns according to published data may be briefly summarized thus^(9,10):

* In later, more detailed, investigations by Kvartskhava of this phenomenon, these channels are referred to as 'E-fibres'.

(1) the blob parameters and the efficiency of the gun are essentially determined not only by the mass of the gas but also by its distribution over the length of the accelerating electrodes;

(2) during the actual acceleration the velocities of the particles forming the blob are not monochromatic but vary widely between 10^6 and 10^8 cm/sec. The highest velocities are those of the ionized particles, which are often multiply-charged ions of atoms released from the walls or the electrodes. They are specially numerous when small quantities of gas are admitted into the gun;

(3) plasmoids, generated by coaxial guns under all conditions of operation, include three characteristic regions: the ionized gas region, the impurity region and a region containing predominantly neutral gas;

(4) in the first region, particle densities may reach values up to $10^{14} - 10^{15}$ cm⁻³, and the velocity up to $5 \cdot 10^7$ cm/sec. In certain conditions, its energy may be equal to 30% of the total energy of the plasmoid. The impurities have smaller velocities. In the third region, characterised by an immense brightness, the particle density attains $5 \cdot 10^{15}$, the velocity $(1 - 6) \cdot 10^6$ cm/sec. The main contribution toward its radiation is supplied by the lines due to the excited neutral gas (hydrogen, deuterium); both this and the second part of the blob are not suitable for plasma experiments.

(5) when the inner electrode is negative the piston formed is more compact and the blob has a higher energy.

Investigations carried out recently have also shed some additional light on the operation of coaxial guns.

Timofeev, Marinin, Shevchuk and Kalmykov (Ukrainian Physico-Technical Institute) measured by mass-spectroscopy the energies of particles in blobs obtained by varying the length of the inner electrode (dia. 2 cm) of a coaxial accelerator, with a view to determining the optimum conditions for the generation of fast particles. The apparatus used is described in reference 11.

The blobs produced by the gun were passed through a glass tube of dia. 10 cm. The mass spectrograph was located at a distance of 1.5 m from the gun.

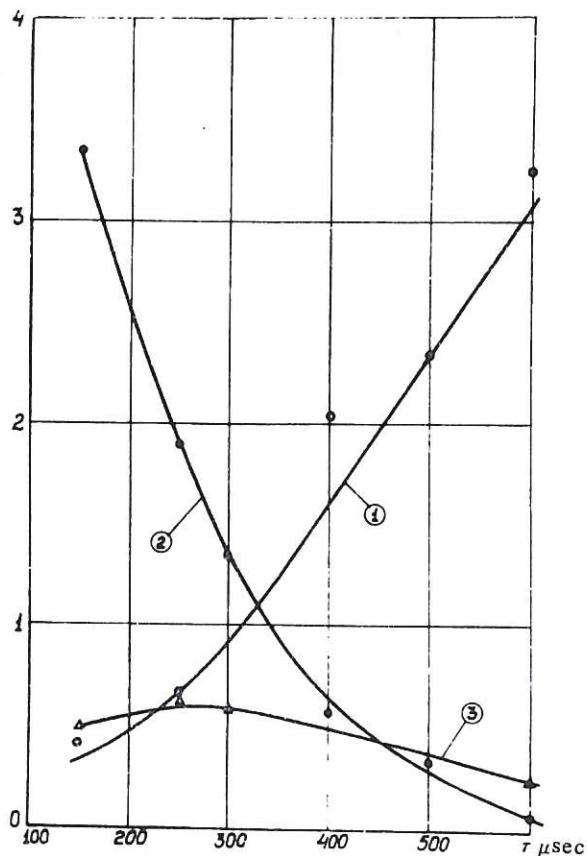


Fig. 1 (CLM-Trans 3)
Amount of impurities against delay τ_d , positive central electrode of length 14 cm
1 - hydrogen, 2 - iron, 3 - fluorine

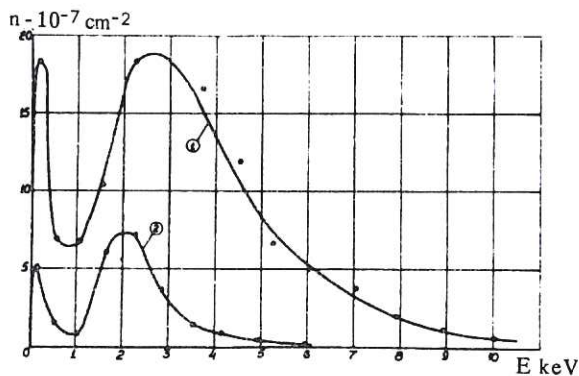


Fig. 2 (CLM-Trans 3)
Energy distribution of hydrogen ions for $\tau_d = 220 \mu\text{sec}$, positive centre electrode of length ℓ where
(1) $\ell = 3 \text{ cm}$ and (2) $\ell = 14 \text{ cm}$

The hydrogen, iron (electrode material) and fluorine (insulator) content in the blob for different delays (τ_d) between the admission of the gas and the connecting of the capacitors, is shown in Fig.1 in relative units.

For small delays the gun (central and outer electrode of the same length - 14 cm) ejects a blob with large iron and smaller hydrogen content.

The curves in Fig.2 show the energy distribution E_i of the hydrogen ions for different lengths ℓ_1 of the positive centre electrode. E_i increased markedly when the electrode length was reduced to 3 cm. In this case, as is well known (refs. 12,15,5,6) the centre electrode is extended by the plasma filament at the boundary of which a characteristic current spiral is formed. A similar spiral and filament are also observed for curve 2 (Fig.2) but only during the final accelerating stage as the blob leaves the gun.

The authors attempted to determine the variation of the mean energy of the hydrogen ions, assuming that acceleration is completed after the passage of the blob through a length ℓ . The inner electrode was positive.

The curves in Fig.3 show (1) that for some value of l the mean ion energy attains a maximum, (2) qualitative agreement between the experimental and the theoretical data, curves 2 and 3, (see reference 8), (3) that the results based on the scheme given in⁽¹⁾ are too high (curve 1).

The agreement referred to should not, however, be overestimated, for the authors failed to take into account in their analysis that acceleration of the plasma in fact continues beyond the inner and, in some cases, also beyond the outer electrode. This effect will be considered in slightly greater detail below.

As mentioned earlier, the quantity and initial distribution of the neutral gas injected into the gun has an important effect on the velocity and purity of the plasma.

Goncharenko, Derepovskii and Konovalov (UFTI) investigated gun performance by regulating the initial gas distribution by means of the gas pressure underneath the inlet valve.

The parameters of the equipment were: $C_0 = 1 \mu\text{F}$; $V_0 = 15 \text{ kV}$; $T = 1.5 \mu\text{sec}$; length of gun 25 cm, electrode diameters 7.9 and 3.2 cm. The gas was admitted at a point 17.5 cm from the gun muzzle.

The mass-spectrograms show that, for a delay of 190 - 280 μsec between the admission of the gas and the breakdown of the discharge, the impurity content was considerably reduced. At pressures under the valve of 6 - 8 atm. the hydrogen content in the blob was 90 - 92%. The velocity of the blob shows some weak dependence on the valve operating conditions and fluctuates between $(2 - 3) \cdot 10^7 \text{ cm/sec}$.

The chosen conditions of gas admission favour formation of a more compact plasma piston and improve gas capture.

The same authors also studied the effect of the direction of the gas jet emitted from the valve into the working volume of the gun. It was found that the hydrogen ions and impurities have the broadest energy spectrum when the gas is injected in a direction opposite

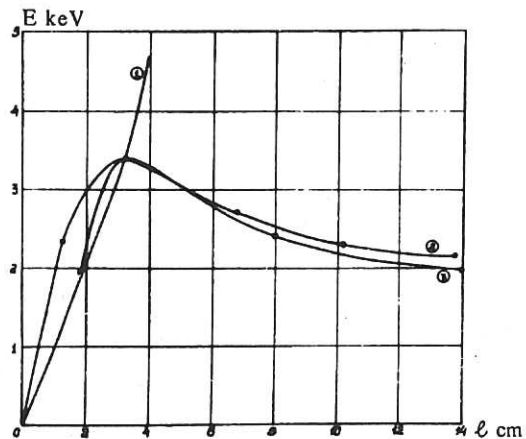


Fig. 3 (CLM-Trans 3)
Variation of mean hydrogen ion energy ν length of (positive) central electrode. (1) calculated from [1], constant gas mass $1.6 \cdot 10^{-6}$; (2) experimental curve $\tau_d = 230 \mu\text{sec}$; (3) calculated from [8]

to the direction of acceleration of the blob. The mechanism of this process is not fully understood; it is possibly related to a decrease in the quantity of injected gas. In these conditions a continuous distribution of the ion spectrum almost up to 70 keV is observed. By injecting the gas in the opposite direction the energy spectrum was limited by a level of 2 keV.

Zolototrubov, Kiselev and Novikov (UFTI) in an attempt to explain the reasons for the development of fast blobs, investigated the current distribution and the motion of the plasma structures within a coaxial gun. Their apparatus differed from that used previously by the length of the coaxial electrode (66 cm) and the system of admission of the gas, which was not pulsed into the working volume from the central electrode (dia. 3 cm) but through an orifice in the outer electrode of diameter 6.5 cm.

The parameters of the capacitor bank were $V_0 = 20$ kV, $C = 12 \mu\text{F}$, $T = 8 \mu\text{sec}$, and hydrogen gas was used.

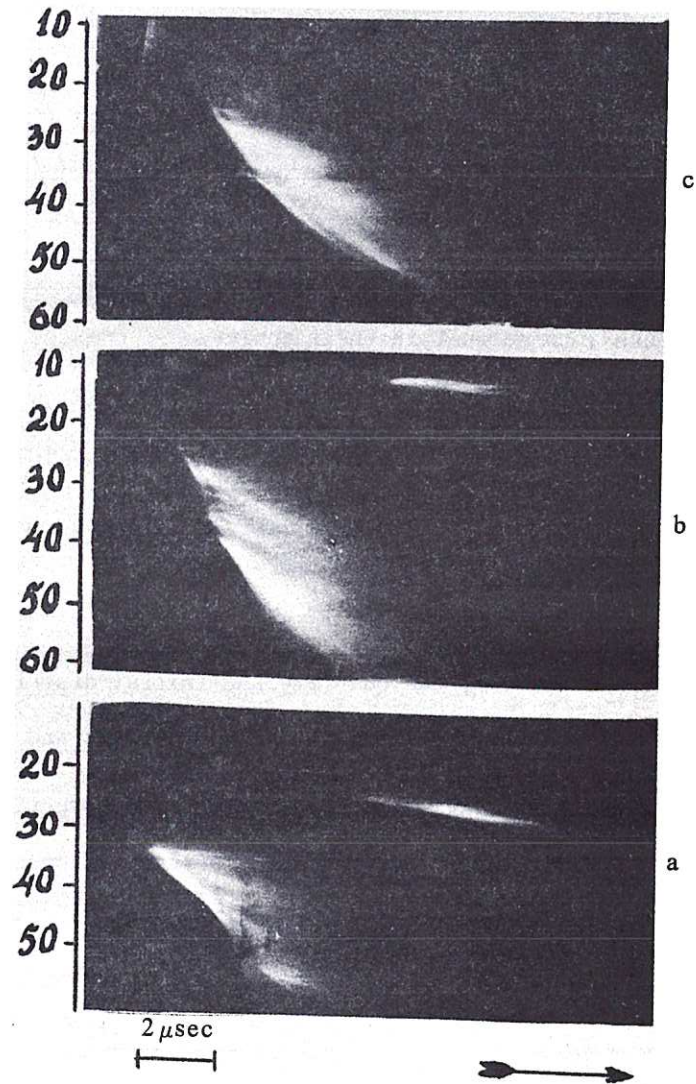


Fig. 4 (CLM-Trans 3)
Streak photographs of discharge in the gun: (a) $\tau_d = 10 \mu\text{sec}$; (b) $\tau_d = 200 \mu\text{sec}$; (c) $\tau_d = 300 \mu\text{sec}$. On the left: distance from insulator in cm. Arrow indicates sweep direction

The current distribution along the gun was measured by differential magnetic probes at the point at which the coils were located. Streak photographs of the light emission through a longitudinal slit in the outer electrode are shown in Fig.4 for different τ_d values. The onset of the discharge coincides with the point of injection of the neutral gas. Figs.4(b) and 4(c) show clearly the formation of several current channels which are displaced relative to one another. The formation of the skin layer is accompanied by a displacement of the luminous boundary toward the insulator.

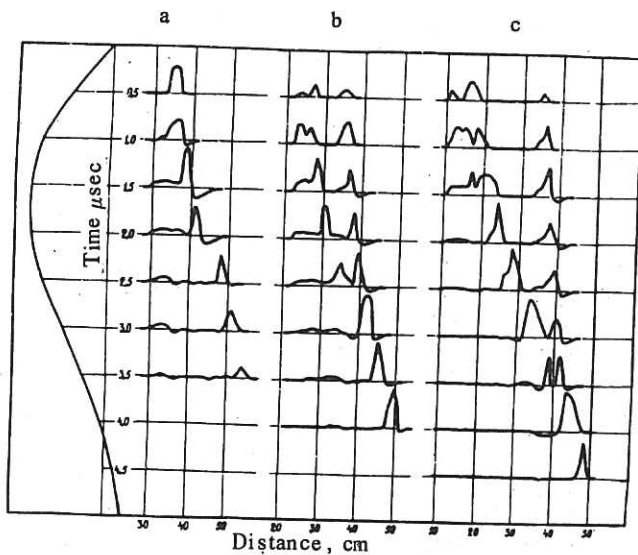


Fig. 5 (CLM-Trans 3)
 Current distribution over the length of the gun with the following delays: (a) $\tau_d = 100 \mu\text{sec}$; (b) $\tau_d = 200 \mu\text{sec}$; (c) $\tau_d = 300 \mu\text{sec}$
 On the left: the currents corresponding to the given distribution

It is worth noting that for a delay of $100 \mu\text{sec}$ the velocity of the first blob is seven times that of the current layer. The velocity of the second blob coincides with that of the current layer.

The authors do not relate the acceleration of the first blob to an electrodynamic process but to drift of the particles behind the current layer in the \vec{E}, \vec{H} fields.

During the first quarter period,

when the particles drift in the direction in which the current layer moves, they may penetrate through the layer and, emerging from the azimuthal field region, may continue their linear motion with a velocity equal to that of their rotation around the Larmor orbits.

In support of this hypothesis they draw attention firstly to the spreading of the luminous intensity in a direction opposite to that of the acceleration of the plasma behind the current layer during the second quarter period, when the induced field \vec{E} changes its sign and, secondly, to the fact that, at a velocity of the blob of $7 \cdot 10^7 \text{ cm/sec}$, $H = 8 \text{ kOe}$,

For $\tau_d = 100 \mu\text{sec}$ the velocity increases sharply near the current maximum.

The results of the probe measurements (Fig.5) agree with these observations and, in particular, indicate the presence of a channel structure. The inhomogeneities in the distribution of the current, which is dispersed over the entire electrode length, are distinctly visible.

Fig.6 compares the velocities of the current layer in the gun muzzle and those of the blobs beyond this region.

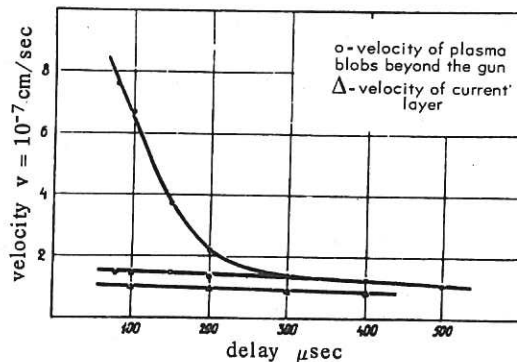
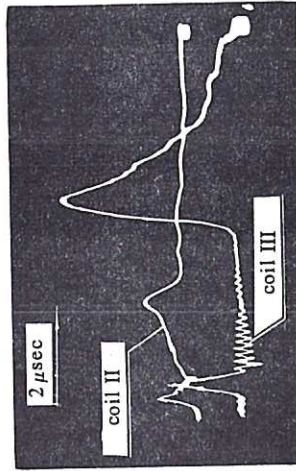
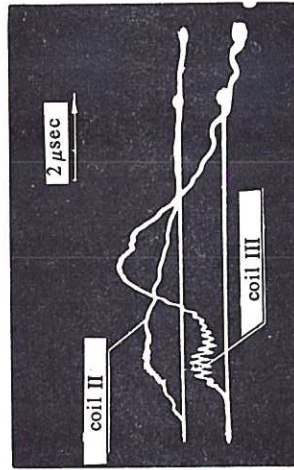
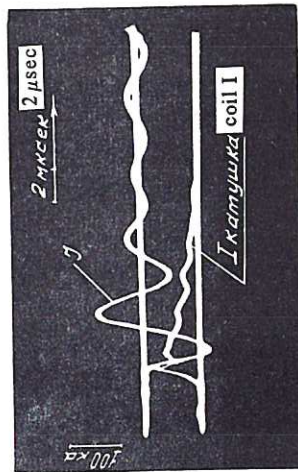
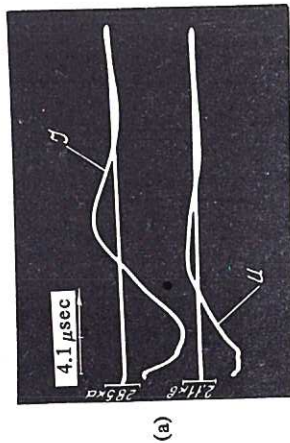
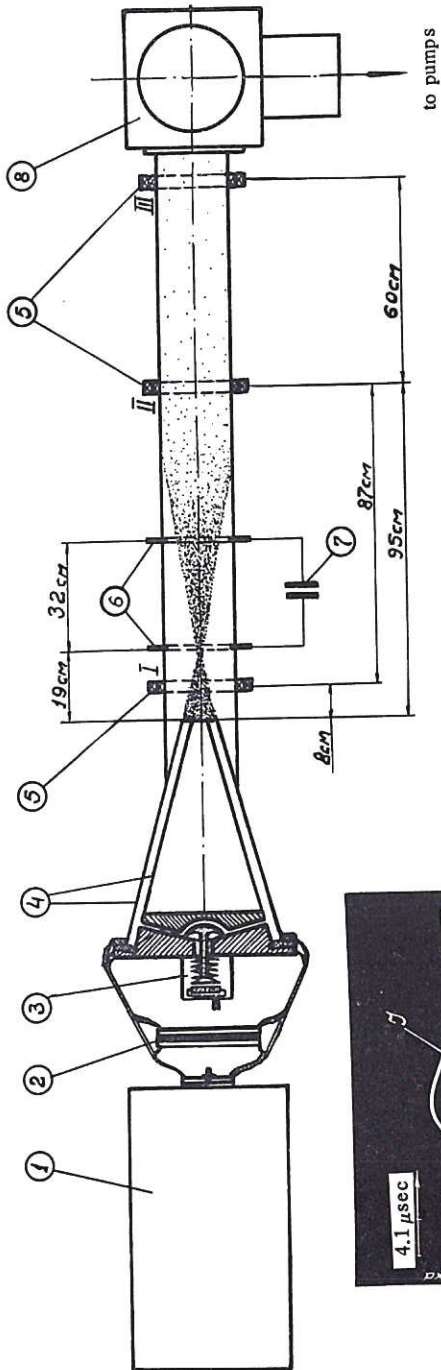


Fig.6 (CLM-Trans 3)
 Velocity of plasma blob and current layer, versus delay

Fig. 7
 (CLM-Trans3)
 Conical gun - scheme. 1 - capacitor bank $C = 750 \mu\text{F}$. $V_0 = 5 \text{ kV}$.
 2 - vacuum spark gap; 3 - pulsing electro-dynamic valve; 4 - conical
 accelerating electrodes; 5 - measuring coils; 6 - second cascade
 ring electrodes; 7 - second cascade capacitor bank, $C = 6 \mu\text{F}$,
 $V_0 \leq 50 \text{ kV}$; 8 - measuring volume. (a) oscillograms of gun current
 and voltage; (b) diamagnetic probe signal from coil I, and cascade
 current; (c) diamagnetic probe signals from coils II and III, cas-
 cade not connected; (d) as in (c), with cascade connected



(a)

(b)

(c)

(d)

the diameter of the Larmor rotation does not exceed the length of the gap between the electrodes.

This hypothesis requires, however, more detailed examination and experimental support, for instance by simultaneous measurement of the E and H fields, comparison of the instant corresponding to the formation of fast blobs with the maximum of their drift velocity which varies with dH/dt . Existing data⁽¹⁰⁾ indicate, first, that the limiting attainable energies in the blob considerably exceed the potential at the source and, consequently, the limiting possible energies attainable during the drift; secondly, that the first blob is generated during 0.2 - 0.3 μ sec, that is, roughly in the middle of the first quarter period.

2. COAXIAL GUN WITH PLASMA FOCUSING

One of the shortcomings of cylindrical coaxial guns is the drop in current density in the forward moving current layer during the second quarter period when the plasma piston approaches the muzzle of the gun. In systems with conical electrodes, as investigated by Komelkov, Drobiazko and Azizov (Institute for Atomic Energy), this shortcoming is partly overcome; as the inductance per unit length increases the gap cross-section decreases toward the muzzle. The break-up of the current piston into separate channels is slowed down and the gas capture improved.

Introducing into the usual mathematical schemes given in⁽¹⁾ a term taking into account the variation of the inductance with length

$$L = L_0 + B_1 x + B_2 x^2$$

where

x is the coordinate over the accelerator length

L_0 the initial circuit inductance

B_1 initial inductance per unit length of the electrodes

and

$B_2 - k - m$ describes the variation of the inductance per unit length,

the optimum conditions for acceleration of the plasma can be calculated. As estimates show, to increase the efficient utilization of the energy put in, it is necessary for L_0 to be minimum, and for $\frac{dL}{dx}$ to be an increasing function.

The type of conical coaxial accelerator with pulsed gas admission (Fig.7) under investigation had the following dimensions: length of accelerating electrodes 65 cm; diameter of inner and outer electrode ends at the accelerator muzzle 3 cm and 11 cm respectively; angle of convergence of the electrodes 16° .

Calculations show that such systems gain by 15 - 20% in efficiency compared with cylindrical coaxial electrodes, without consideration of the circuit resistance, and by 5 - 10% with its consideration. As apparent from curve 1, Fig.8, the highest ratio

$$q = \frac{B^2 C^2 V_0^2}{2 m L_0} = 10,$$

of the kinetic energy of the accelerated plasma to the energy stored in the capacitor bank, is obtained from the dimensionless parameter q where C is the bank capacitance, (μF), V_0 the capacitor voltage in volts, and m the accelerated mass of plasma in kg.

The highest q value obtained in the experiments described below, was 3 - 4, and the closest approach to the theoretical curves was achieved.

Two kinds of gas were used, namely, air and hydrogen at different initial pressures P in the electrodynamic valve which had a working volume of 2 cm^3 . The efficiency of transfer of the capacitor bank energy to kinetic energy of the plasma is also demonstrated by the strong damping of the current in the discharge (Fig.7). The maximum current in the gun was 600 kA. When passing from air to hydrogen the discharge duration was extended, the

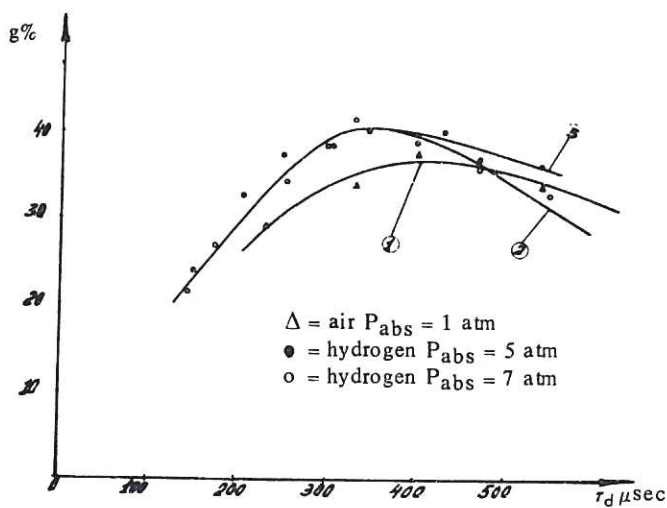


Fig. 9 (CLM-Trans 3)
Energy transferred to plasmoid, ν delay in switching on capacitor bank

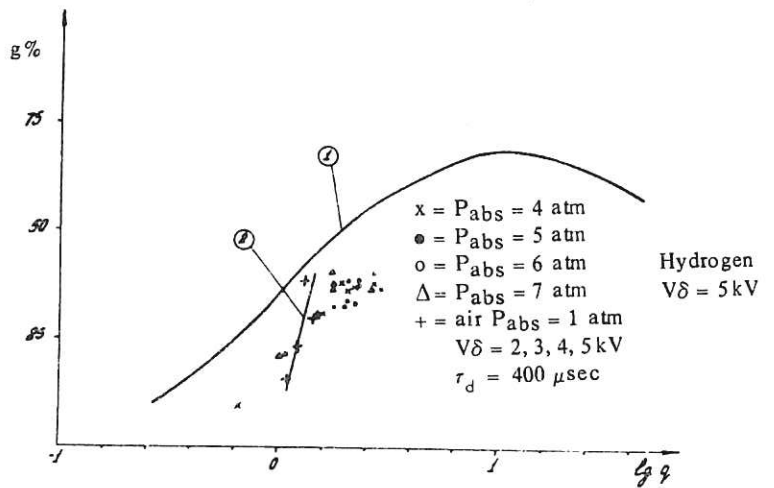


Fig. 8 (CLM-Trans 3)
Efficiency of acceleration against q

current amplitude decreased. The energy of the plasma blob was measured by a calorimeter, its momentum by a pendulum.

The time τ_d elapsed between the start of the admission of the gas and the switching on of the capacitor bank has a significant effect on the efficiency of the energy transfer to the plasma. Fig. 9 shows a plot of $g = f(\tau_d)$, which has an optimum at $\tau_d = 320 \mu\text{sec}$ for hydrogen, and $\tau_d = 400 \mu\text{sec}$ for air.

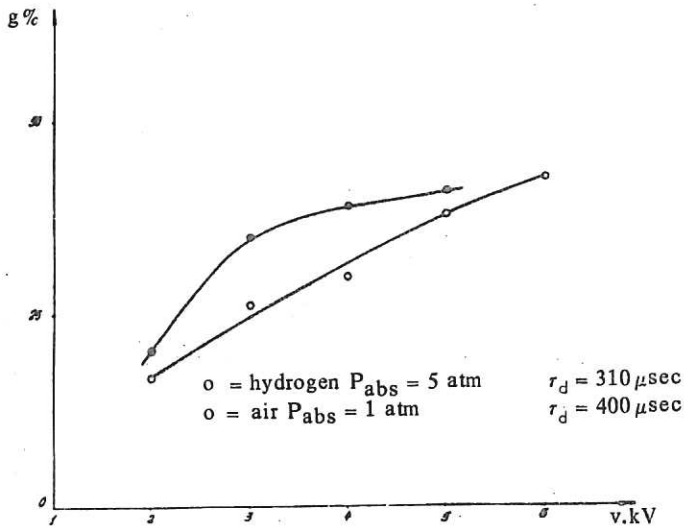


Fig. 10 (CLM-Trans 3)
Energy transferred to plasmoid for optimum τ_d ,
for different capacitor bank voltages

The conditions for the formation of the plasma piston are related to an optimum current density in the piston or an optimum total discharge current.

Fig. 10 shows the increase in efficiency of the energy transfer to the blob with the capacitor bank voltage. For hydrogen at 3 kV the value of g obtained varies only very slightly when V_0 is increased further; for air, this limit was not attained even at $V_0 = 6$ kV.

Measurements of the momentum of the plasmoid under similar conditions showed that when V_0 is increased 2.5 times the mass of air trapped by the plasmoid increases fivefold. An approach to the approximate snow-plough scheme is thus observed over a very narrow interval of pressures at certain electric circuit parameters. An additional reason for the discrepancy between the actual and estimated g values, amongst other things, is that the plasma reaches the muzzle of the gun where it can no longer be accelerated before the current has completely decayed away. This current can, however, be used to some extent for further acceleration of the plasma by lengthening the outer electrode by means of a special extension. With this extension in use, and working with hydrogen, the momentum of the plasmoid increased by 5%, the energy of the blob by 15%.

The plasma jet emitted by the conical gun during the first 7-8 μ sec converges at the geometrical focus of the electrodes; then, whilst the cooler gas flows off, the focus becomes diffuse and moves toward the ends of the electrodes. The diameter of the jet at the focus does not exceed 6 cm. According to the streak photographs, the main brightness is concentrated in a region of diameter 4 cm. The front portion of the jet converges into a beam of diameter 2 cm.

The plasma density at the focus, in a region of radius 2 cm, exceeds the mean density, about 4-8 cm from the axis of the blob, by a factor of about 14. The corresponding factor for coaxial guns is $1.5 - 2^{(13)}$. Conical guns not only make possible an increase of the particle density at the focus but are also suitable for injecting plasma into the narrow

entry channels of thermonuclear devices without the use of external magnetic fields which reduce the velocity of the plasmoid. On the other hand, when traps of large diameter are to be filled with a low particle density, the divergent portion of the jet can be used.

The convergence of the fluxes at the focus leads to a flash of brightness and to additional heating of the plasma. The temperature of the plasma beyond the focus, determined from the velocity of the shock waves⁽¹⁴⁾, is approximately 6 eV.

The frontal velocity of the blobs, measured from the diamagnetic probe signals, varies depending on the quantity of injected gas or the delay τ_d and the gas pressure underneath the valve (Fig.11).

The maximum velocity of hydrogen blobs, $(4 - 6) \cdot 10^7$ cm/sec, was measured for delays corresponding to the formation of separate plasmoids, detached from the main bulk of the gas. In this case the probe signals are several separate pulses. In the region of optimum efficiency one obtains a signal with a steep front, indicating compactness of the plasmoid. The front of the blob is 10 - 15 cm long.

As the blob moves on, a group of fast particles forming its frontal portion, are gradually separated, leaving the neutral particles and the heavy impurities behind. Some increase in the monokinetic character of the particles forming the front, without substantially re-

ducing the velocity of the blob, can be achieved by increasing the pressure P_0 of the gas underneath the valve.

Thus, for $P_0 = 9$ atm. the length of the front, λ_ϕ , at a distance of 95 cm from the muzzle, is 45 cm; at $P_0 = 2$ atm, $\lambda_\phi = 100$ cm.

Fig.12 shows the time lag for carbon, measured from the CII 4267 line at 26 Å for different τ_d values, at the focus of the injector. For small delays the time lag of carbon

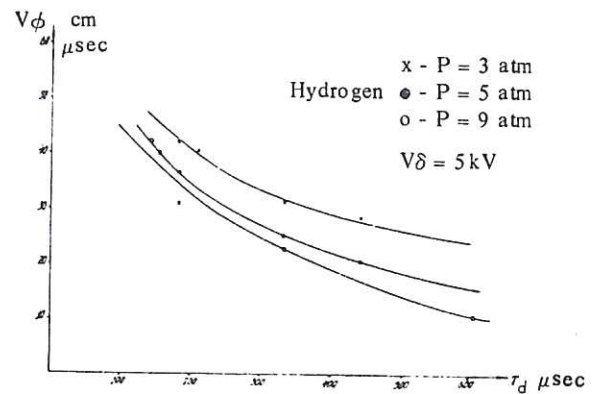


Fig.11 (CLM-Trans 3)
Variation of blob front velocity with τ_d

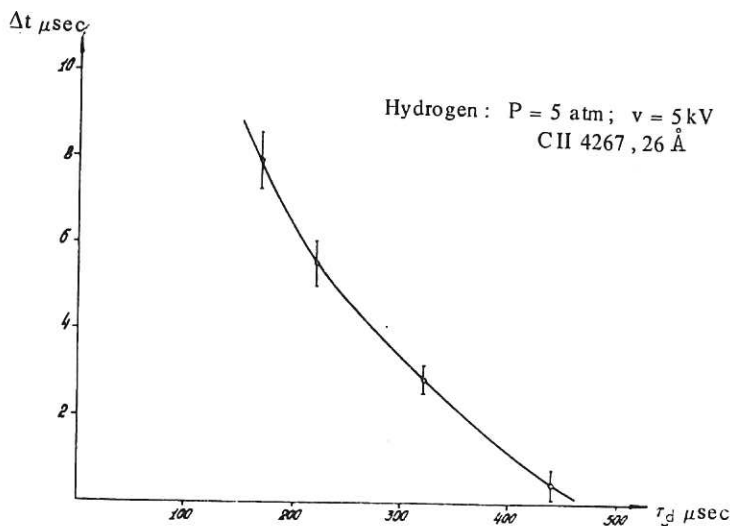


Fig.12 (CLM-Trans 3)
Time lag in the appearance of carbon (CII 4267, 26 Å) at the focus of the jet, for different values of τ_d

is 8 μ sec, in conditions of optimum acceleration 2 - 3 μ sec. This presents a real possibility for removing the impurities from the frontal blob region.

Blob velocities can be increased further either by changing to conditions where $q \geq 10$, or by introducing an additional accelerating cascade. A similar cascade is shown in Fig.7. The accelerating electrodes, in the form of two rings, are connected to a capacitor bank with $C = 6 \mu$ F and $V_0 = 10 - 50$ kV. The discharge of the banks which occurs when the electrodes are short-circuited by the plasma blob has a frequency $f = 220$ kc/s. Compression and ejection of the plasma take place both in the same and in the opposite directions to that of the blob. The front of the plasmoid accelerates, the tail slows down. The oscillographs on Fig.7 represent:

- (1) the signal from the diamagnetic probes III and IV with and without the cascade on;
- (2) the cascade current.

The point of breakdown of the bank is determined by its voltage, the electrode gap and the τ_d of the injector. The most favourable point was $\tau_d = 450 \mu$ sec, $P_0 = 3$ atm.

Table I shows the results of provisional measurements of the velocities of the frontal blobs between the diamagnetic probes III and IV.

TABLE I

Cascade voltage, kV	0	10	20	25	30
Velocity of blob front between coils, III and IV, cm/sec	2.9×10^7	3.3×10^7	$(5.5 - 8.6) \times 10^7$	$(8 - 15) \times 10^7$	4.3×10^7

The maximum velocities, in excess of 10^8 cm/sec, were obtained at $V_0 = 25$ kV. From approximate estimates the density of the plasma, at the instant corresponding to the maximum on the diamagnetic loop signal, is $5 \cdot 10^{15} - 10^{16}$ cm^{-3} , at a distance of 50 cm from the focus. The density at the focus attains values of 10^{17} cm^{-3} .

In the frontal plasmoid, with the cascade on, the density is $5 \cdot 10^{14} - 10^{15}$ cm^{-3} .

3. BOSTICK TYPE GUNS

It has been shown earlier^(5,15) that in systems with coaxial electrodes plasma acceleration processes still go on even after the plasma has passed beyond the limits (ends) of the electrodes if the current flowing in the external circuit is not cut off at this moment. This process, referred to as 'fountain pinch', is especially marked in an accelerator with limitingly shortened electrodes of the ring-pin or the ring-ring types. In one variant of

this plasma source the pin and the ring are of different lengths and the interspace is filled with an insulating cone. In such systems a plasma jet is characterised by:

- (1) the formation of a dynamic plasma filament forming an extension of the pin electrode, and an external coaxial plasma connected to the ring electrode;
- (2) the twisting of some of the current in the filament into a spiral, and the formation of a longitudinal magnetic field;
- (3) prolonged X-radiation and a continuum radiation from the current filament;
- (4) the breaking up of the jet into separate plasmoids, which retain the same structure.

In addition, the Bostick type gun was also investigated by Osher⁽¹⁶⁾ who was, however, only interested in its resultant characteristics, and did not consider the intrinsic currents of the blobs which play an important part both in the acceleration and in the interaction of the blobs with the magnetic fields.

Komelkov, Skvortsov, Tereshenko (IAE) studied the formation of current plasmoids, using equipment described in⁽⁷⁾, in a glass tube of length 1.5 m and inner diameter 18 cm. The outer diameter of the pin electrode and the inner diameter D of the ring electrodes were 5 and 10 cm respectively. The gas was admitted at a point near the end of the ring electrode. Two characteristic sets of operating conditions were compared: one using a large load of gas admitted from the valve with $\tau_d = 150 \mu\text{sec}$, and 'small gas load' conditions with $\tau_d = 50 \mu\text{sec}$. The hydrogen pressure in the working volume of the valve, which has one cubic centimetre, was 4 atm.

The period of the oscillations of the discharge current was 19 or 30 μsec , depending on whether the capacitance of the bank was 36 or 144 μF .

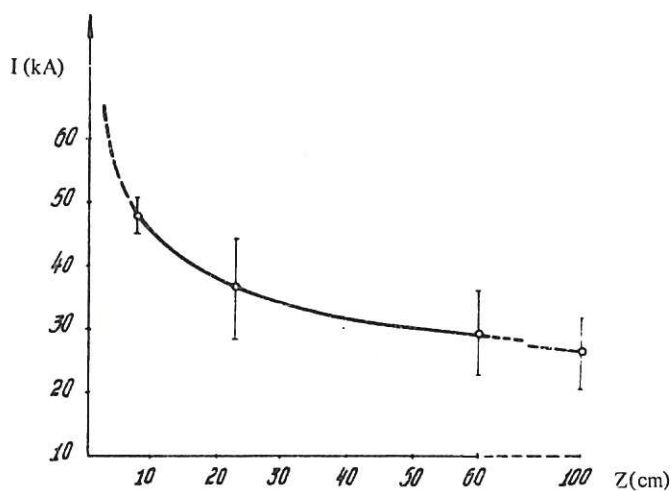


Fig. 13
(CLM-Trans 3)
Maximum current of plasmoid for different distances
 $Z(\text{cm})$ from the ends of the electrodes

Under 'large gas load' conditions the current distribution in the jet was very similar to that observed under continuous filling conditions^(5,15). In the first case the current flowed well outside the electrode region. According to the probe measurements in the H_ϕ field plasmoid currents of about 30 kA were measured at a distance of about one metre from the electrodes (Fig.13) at $l/D \geq 5$ (l being the length of the current channel).

The current drop is largest 20 cm from the electrode ends, in the region originally filled with neutral gas and then with electrode vapour. With the increasing amount of electrode vapour the current concentrates increasingly in the vapour, and the separation of the frontal portion of the jet from the main bulk occurs with relatively small currents. When the capacitor bank voltage is increased

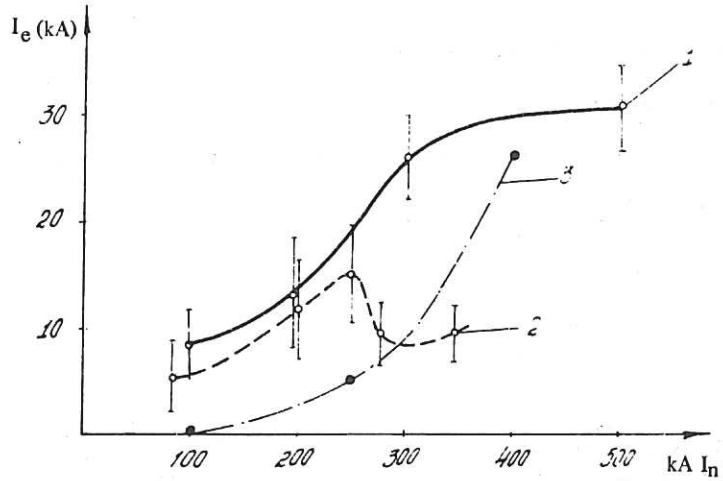


Fig. 14 (CLM-Trans 3)
Currents in plasmoid for $Z = 100$ cm, as a function of the total discharge current. 'Large gas load' conditions

- Curve 1 - $C = 144 \mu\text{F}$; $H_{z \text{ ext}} = 0$;
- Curve 2 - $C = 36 \mu\text{F}$; $H_{z \text{ ext}} = 0$;
- Curve 3 - $C = 36 \mu\text{F}$; $H_{z \text{ ext}} = 10 \text{ kOe}$

one observes that in conjunction with the total current I_n the current in the plasmoid I_e , as apparent from curve 1, Fig.14, increases only up to a certain not very high limit. This is followed by saturation, and at a smaller bank capacitance (curve 2) a drop of I_e occurs due to the increasing electrode evaporation.

The signals due to the H_ϕ field and the longitudinal H_z field, indicating the existence of the above mentioned structure in the plasmoid, remain the same over the total

length of the plasma column. In a number of cases, 2-5 separate signals are received corresponding to the separate blobs into which the plasma jet breaks up.

In 'small gas load' conditions the current and voltage oscillograms show a discontinuous character (Fig. 15) which is related to the repeated breakdowns and acceleration cycles which are renewed after ejection of the plasma over a length of 20-30 cm.

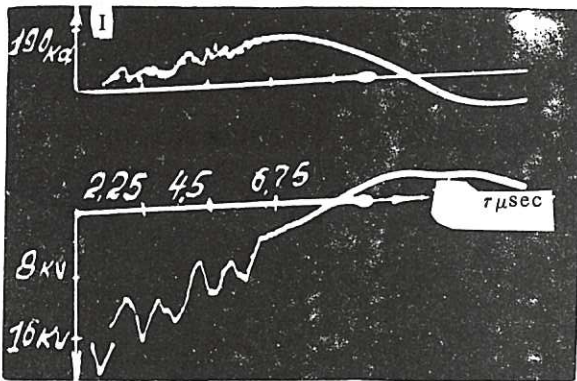


Fig. 15 (CLM-Trans 3)
Oscillograms of current and voltage for Bostick type gun in 'small gas load' conditions ($\tau_d = 50 \mu\text{sec}$)

According to the probe measurements, approximately 80% of the total discharge current flows in each such blob. After a distance of 15-20 cm a considerable transformation of the probe signals is observed which gradually degenerate into high frequency oscillations with a frequency up to 50 Mc/s.

The signals due to the H_ϕ field are no longer screened by the outer coaxial plasma and penetrate outside the chamber. It appears as though the plasmoid breaks up into separate current filaments with continually varying position and orientation, a phenomenon conceivably due to a beam instability of a type as yet insufficiently investigated.

High speed photographic recordings obtained in 'large gas load' conditions (Fig.16) indicate that when ejected into a vacuum the front of the jet is flat rather than conical

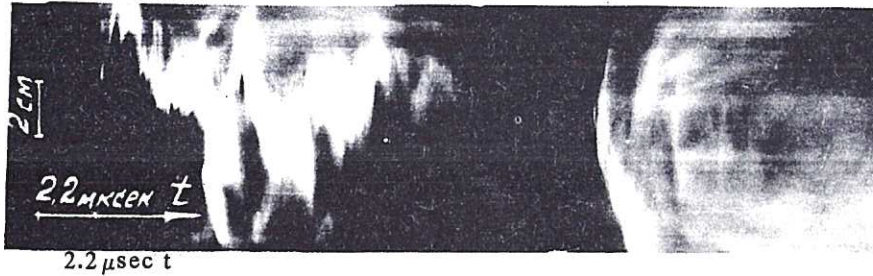


Fig. 16
Streak photograph of plasma jet taken through a transverse slit located at a point 25 cm from the electrodes

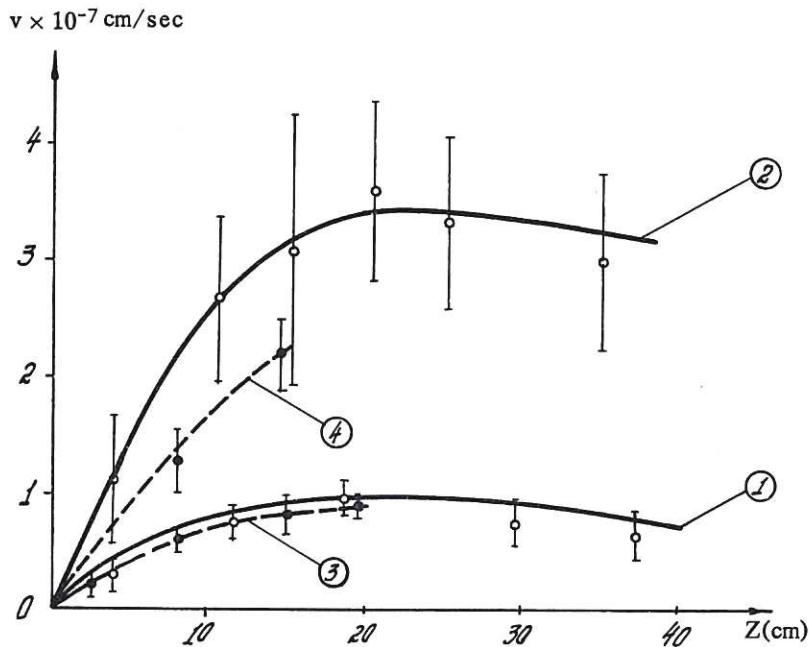


Fig. 17 (CLM-Trans 3)
Velocity of current fronts in a Bostick type gun (curves 1, 2) and a coaxial gun (curve 3, 4)
Curves 1 and 3 $\tau_d = 150 \mu\text{sec}$
Curves 2 and 4 $\tau_d = 50 \mu\text{sec}$

are the high absolute values of the velocities $V = 4 \cdot 10^7$ cm/sec which are usually obtained in coaxial guns whose inductance is negligible compared with the present case.

The velocities of the frontal particles, forming a current-less blob, are higher still, attaining values (according to diamagnetic probe measurements) of $(6 - 7) \cdot 10^7$ cm/sec.

as in the second half period when the chamber is filled with gas (see also⁽⁷⁾). The current filament spiral appears 4-5 μsec after the start of the discharge. The amplitude of its oscillations from wall to wall attains values of 8-10 cm.

Fig.17 shows current front velocities at $\tau_d = 150 \mu\text{sec}$ (curve 1) and $\tau_d = 50 \mu\text{sec}$ (curve 2). The increase in velocity of the blob occurs over the first 20 cm of its path in the maximum current region. Beyond this region it remains virtually unchanged. Of interest

The conclusion may therefore be drawn that the most suitable conditions from the point of view of obtaining plasmoids of high velocity exist in the 'low gas load' regime, in which the duration of the accelerating cycle is only 1 μ sec, and the discharge currents attain values of 30 - 40 kA. To work in these conditions it is unnecessary to have capacitor banks of high capacitance, since they can in fact be obtained using coaxial lines.

The appearance of impurities in the discharge was determined by means of image converter photographs of the jet obtained in the light of the Cu II $\lambda = 4690 \text{ \AA}$ line. Copper atoms appear at the end of the electrode ($V_0 = 15 \text{ kV}$, $C = 36 \text{ } \mu\text{F}$, $I = 120 \text{ kA}$) 5 μ sec after the onset of the discharge. Their mean velocity is $4 \cdot 10^6 \text{ cm/sec}$. As the voltage is decreased to 3 kV no copper lines are observed at a distance of $z = 50 \text{ cm}$ even with intensification. Going over to these conditions constitutes one approach towards obtaining a relatively clean plasma.

In operating conditions with large currents, the entry of impurities into the discharge can be prevented by short-circuiting the capacitor bank at the instant at which the discharge currents reach values of 50 - 60 kA/cm². An effective method of suppressing the break-downs occurring during the second and the following half-periods, might be the introduction into the discharge circuit of a non-linear 'Vilit' resistance as suggested by Zaients, Nikolaevskaya and Shneerson, or by short-circuiting the capacitor bank at the end of the first half period.

The blob can be isolated from the walls by means of a longitudinal magnetic field. A plasmoid carrying a current of 12 kA moves very stably through a solenoid of 80 cm length situated 40 cm from the gun electrodes, since a system of two mutually perpendicular fields is formed by H_ϕ and $H_z \text{ ext}$, as in the 'Levitron' (37).

In a field of 10^4 oersted the blob diameter is roughly halved; at small currents the blob is slowed down strongly on entering the magnetic field.

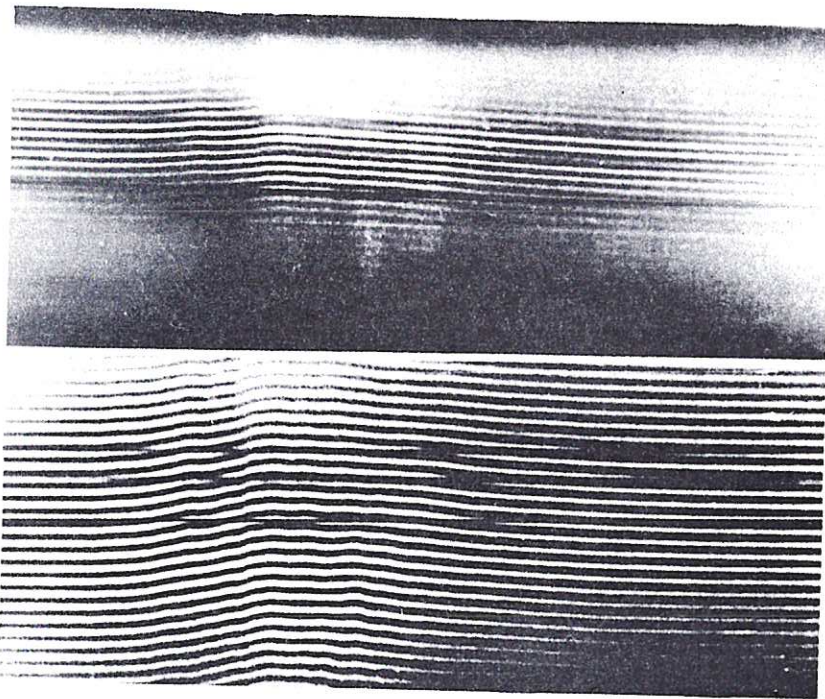
It is worth noting that in a blob moving in longitudinal fields the currents are larger than in a blob moving freely, without fields. The reason is partly that the flux of neutrals from the walls to the centre of the blob has stopped and partly the compression of the blob on entering the magnetic field.

Due to the characteristic structure of the magnetic fields and radial currents, fast particles and blobs are generated more effectively in Bostick type guns than in coaxial guns.

Comparative experiments were carried out with coaxial guns of a length (22 cm) and electrode diameter (5 and 10 cm respectively) chosen in accordance with calculations of the type given in (1). The external circuit parameters and the gas inlet conditions remained the same.

Under 'large gas load' conditions the velocity of the blob was found to be similar as in the Bostick gun (curve 1, Fig.17). Under 'small gas load' conditions the velocity of the current front was double in the case of the coaxial gun (curve 4, Fig.17).

We mentioned earlier on, firstly, that as V_0 increases the extension of the current beyond the electrodes H_z and $\partial H_z/\partial t$ increases and, secondly, that with the field geometries and current structures described, hard X-radiation (100 - 200 keV) from the region of the current filament is observed which is due to electrons obviously accelerated in the eddy electric fields^(5,15).



The formation of current eddies and the extension of the current beyond the electrodes undoubtedly also occur in other guns, in particular in conical guns.

Borzunov, Orlinskii and Osovets⁽¹⁸⁾ proposed so-called conical chambers with a view to obtain cumulation in powerful discharges and toward its use for heating the plasma by colliding jets.

Scott and Voorhies⁽¹⁹⁾ used the same cumulation concept and the same electrode configuration (pin at apex of an insulated cone, rings at its base); a similar gun was later also investigated by Azovskii et al⁽¹⁷⁾. It was shown experimentally⁽¹⁸⁾ that a process resembling cumulation occurs in the region of the conical chamber. However, as the plasma passes beyond

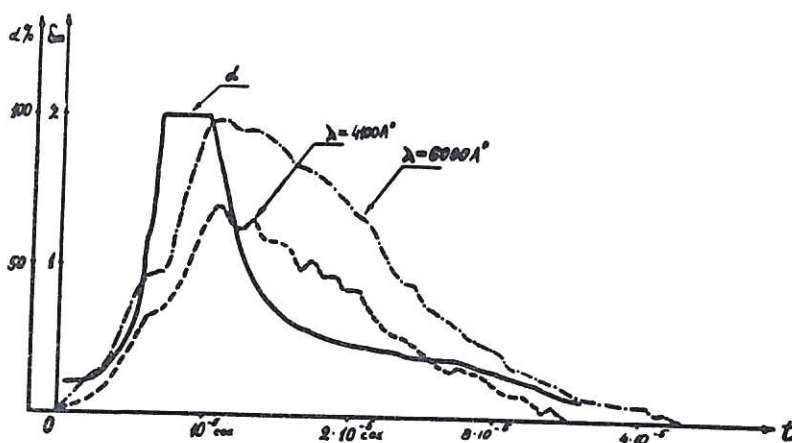


Fig. 18
(CLM-Trans 3)
Interferometer diagrams of a plasmoid from a conical gun taken in the light of the $\lambda_I = 6000 \text{ \AA}$ and $\lambda_V = 4000 \text{ \AA}$ line.
Below, the line profile and a plot of $\alpha = f(t)$

the ring, electrode acceleration changes to the Bostick gun conditions, with formation of current plasmoids.

In various investigations on the subject of shock tubes, accelerators and guns the presence is reported of a current filament, or of magnetic field characteristic of the structure mentioned. However, the authors are often unaware of the causes of these phenomena⁽¹⁷⁾.

Kruglyakov and Nesterikhin (Institute of Nuclear Physics) studied blobs obtained from a conical gun (ring diameter 3.3 cm, pin-ring spacing 6 cm; $V_0 = 3-4$ kV; $C = 16 \mu\text{F}$). The working material in the gun was supplied by the dissociation products of the perspex, the material of the insulating cone. Interferometric resolution of the blob photographed through a transverse slit in the light of the lines at $\lambda = 4100 \text{ \AA}$ and 6000 \AA permitted the simultaneous observation of the light emission of, and of the particle density distribution in, the blob; the appearance of the spiral current filament and its oscillations in the tube is exactly the same as in the 'fountain pinch' (Fig.18).

Graphs are reproduced below showing the displacement δ_m of the interference fringes from which the degree of ionization α was determined.

For the given blob dimensions (dia. 3.3 cm) the electron concentration can be determined from:

$$n_e = 5.6 \times 10^{16} \delta_m .$$

The records show that the maximum 100% ionization is not attained at the front of the jet as was expected, but after 8 - 10 μsec .

The results of the mass-spectrometric investigation of the blob composition are given in Fig.19. The first to be recorded are hydrogen ions with energies of 1 - 4 keV,

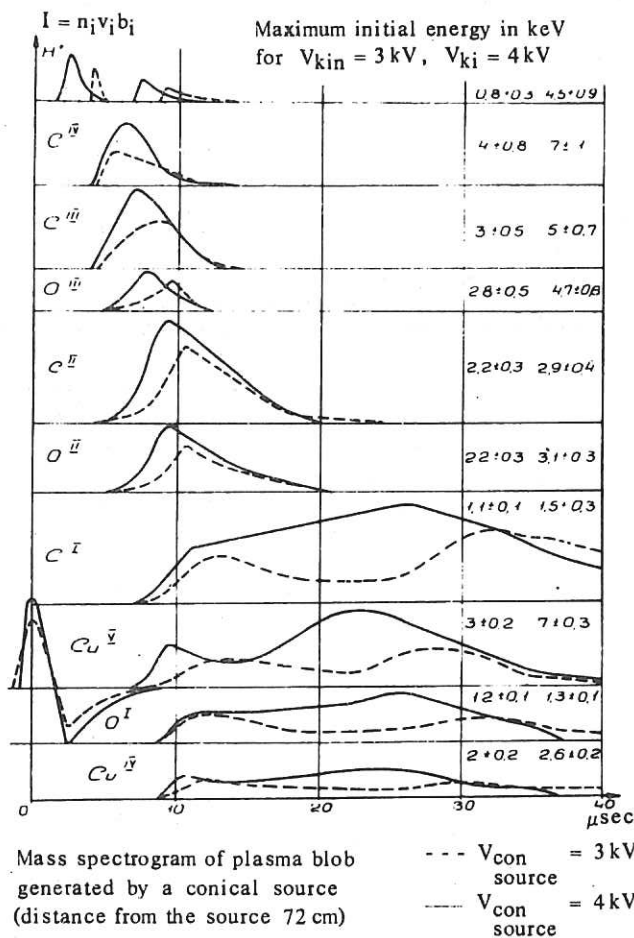


Fig. 19 (CLM-Trans 3)
Mass spectrograms of a plasma blob from a conical source, obtained at a distance of 72 cm from the ring electrode. The current oscillograms are shown preceding the records of the CuV lines

observed in two blobs. The heavier ions arrive later and move in one blob.

The ion energy E_i was found to be proportional to their charge, as verified by the example of carbon, where $E_{CIV} = 4$ keV; $E_{CIII} = 3$ keV; $E_{CII} = 2.2$ keV; $E_{CI} = 1.1$ keV.

As the spectrograms show, the generation of high energy ions takes place over 40 μ sec, whilst the current in the external circuit flows in all for 8 μ sec. This means that in plasmoids ejected by conical guns just as in those from Bostick type guns independent closed currents and accelerating electric fields, forming not only in the front but over the total length of the plasmoid, persist for prolonged periods.

4. TITANIUM PLASMA SOURCE

The titanium plasma source has been used for filling various traps for several years^(20,21). One such source, designed and investigated by Andrukhina and Shpigel (Physical Institute, AN, USSR) is shown in Fig.20. It is made up of twenty previously outgassed and hydrogen impregnated (1:1 at. ratio) titanium discs. The discs are separated by steatite or teflon insulators and located in a steatite box fitted into a stainless steel vessel; inset into the aperture of the first disc is the trigger electrode to which the igniting pulse is

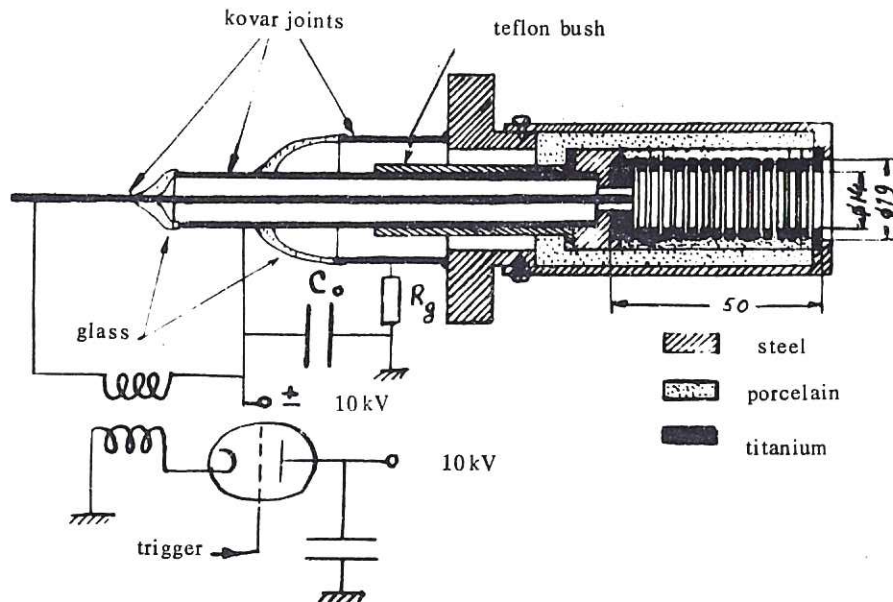


Fig. 20 (CLM-Trans 3)
Schematic of titanium source and supply circuit

applied. The discharge in such a system has not been described in the literature. It may be visualised roughly thus. After applying the voltage to the first and last discs all insulating gaps break down. The skin layer forms first around the insulator surface, then moves toward the axis of the source, heating the surface of the discs and evaporating the hydrogen. After compression of the discharge, during which the gas is partially heated,

the current filament forms at the vessel axis. The rest of the process is probably in many features fairly analogous to that taking place in the Bostick type guns. The generation of large currents is not very probable, because of the unfavourable radial spreading of the currents and the proximity of the walls where secondary breakdowns may develop followed by new pinches and so forth. In the case of a large buildup of hydrogen and metal vapour in the discharge gap and at the relatively small currents normally used in such sources, there is a transition from the conditions of electrodynamic acceleration to those of thermal heating by the discharge currents; sources of this type operate most favourably by short pulses. In experiments by the authors, at a capacitance of the capacitor bank $C = 1.6 \mu\text{F}$, the discharge was damped by a resistance 2ρ or 4ρ ($\rho\sqrt{L/C} = 0.33 \Omega$). The current at the maximum was 5 kA. $T = 3.3 \mu\text{sec}$. Measurements showed that, as in other guns, the protons have the highest velocity and two components were observed with velocities of $4 \cdot 10^7$ and $2 \cdot 10^7$ cm/sec respectively, corresponding to the respective energies of 800 and 200 eV. The proton energy distribution spectrum includes two maxima, at 100 and 600 eV. The C^+ , C^{++} , Ti^{++} ions have energies between 50 - 150 eV, and form the tail of the blob.

The impurities enter the discharge with some time-lag of 0.5 - 0.7 μsec relative to the hydrogen. Switching on the damping resistor ρ leads to a rapid drop in impurities, as is evident from Fig. 21. Measurements of the transverse energy of the ions in the beam gave H^+ transverse energies of 1.2 eV, with corresponding values for Ti^{++} and Si^{++} of about 3 eV, and these were independent of the accelerating potential. The angle of divergence for the H_1^+ ions is smaller by an order of magnitude compared with the angle for heavy

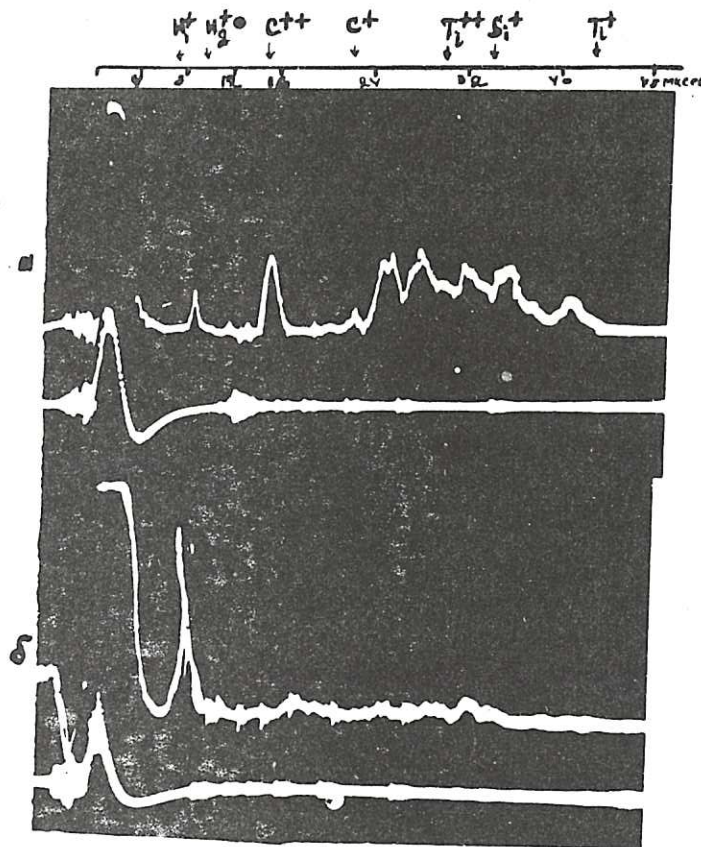


Fig. 21 (CLM-Trans 3)
 Integrated mass-spectrograms of a plasma generated by a titanium source. First beam - mass spectrum, second beam - current in circuit of source. Capacitor voltage 6 kV
 (a) $R = 2\rho = 0.68 \Omega$ (b) $R = 4\rho = 1.12 \Omega$

impurities. This effect can be utilized for cleansing the jet from the heavy ions.

An important source of impurities is the oil vapour from the diffusion pumps, which condenses at the walls and electrodes. When using titanium pumps the hydro-carbon content in the spectrum is considerably reduced.

PART II

MOTION OF PLASMA BLOBS IN MAGNETIC FIELDS

The construction of guns producing pure plasma is closely connected with problems concerning the separation of impurities and neutral particles from the plasma blobs. In addition to investigating gun operating conditions aiming at reducing the amount of impurities getting into the plasma to a minimum, it definitely seems promising to explore further methods of separating neutral atoms and impurities from the pure plasma using magnetic fields of different types and configurations.

Investigations carried out so far in this direction reveal, on the one hand, the complexity of the interaction processes of a multi-component plasma in a magnetic field, whilst on the other they yield information presenting a wider general plasma physics interest, especially as concerns our understanding of the mechanisms underlying the motion of a plasma contained in magnetic traps.

1. MOTION OF PLASMA BLOBS IN LONGITUDINAL MAGNETIC FIELDS

The work of Vasilev, Komelkov, Pergament, Tserevitinov (IAE) constitutes an extension of earlier researches into the motion of blobs in longitudinal magnetic fields^(22,13,23). The plasma blob was obtained from the coaxial gun described in⁽²⁴⁾, with $V = 5$ kV, $\tau_d = 350$ μ sec. The longitudinal magnetic field, set up in the cylindrical plasma guide of 10 cm dia. attained its maximum in 350 μ sec.

A calorimeter, diamagnetic probes, image converters and spectral methods were used to measure the velocity v , the blob diameter d , and the particle density ρ for different distances Z from the gun.

A slowing down of the blob emitted from the gun was observed even before it reached the point of entry of the solenoid, i.e. in the fringing field region. Just as according to^(13,22), v decreases with τ_d . The velocity of the blob remains practically constant within the solenoid, over a distance of 60 cm.

For $H_z = 13$ kOe the velocity of the head of the blob is halved compared with its initial velocity of $2 \cdot 10^7$ cm/sec. The velocity of the intensely bright part of the blob decreased from $8 \cdot 10^6$ cm/sec to $6 \cdot 10^6$ cm/sec. Calorimetric measurements indicate that the diameter of the plasmoid decreases only on entering the magnetic field and changes very little subsequently.

Curve 1 in Fig.22 plots the diameter d , measured calorimetrically, versus H_z . Curve 2 gives the analogous data taken from⁽²³⁾. Curve 3 shows the variation in the diameter of the dark frontal part of the blob, transferring about 30% of the total energy. Here the dependence is more marked and can obviously be associated with the higher degree of ionization and the smaller particle density. The results obtained from measurements of the light emission in the neutral gas-enriched impurity region approximate closely to those of the calorimetric measurements.

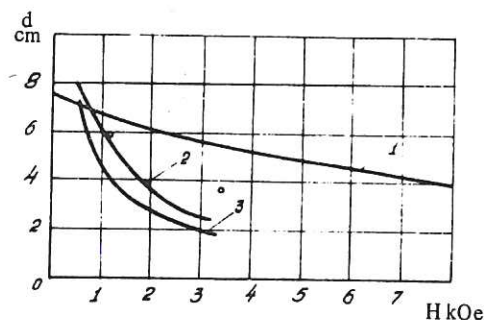


Fig. 22 (CLM-Trans 3)
Diameter of plasmoid v H_z . 1 - calorimetric
2 - diamagnetic probe, distance 10 cm. 3 - diamagnetic probe, distance 20 cm from entry point into coil. O - streak photography

The decreasing amplitude of the diamagnetic probe signal with the distance z , testifies to the diffusion of the magnetic field into the ionized region of the blob; from its velocity (diffusion) conclusions may be drawn⁽²⁵⁾ as to the electron temperature in the plasmoid which, according to estimates, is T_{e1} at $H_z = 200$ oersted*.

From the known temperature the particle density in the blob was determined from the equality of the magnetic and gas-kinetic pressures. The same relationship $\rho = f(H_z)$ could also be obtained from the diameter d (Fig.22) and ρ_0 (for $H_z = 0$; $\rho_0 = 7 \cdot 10^{14}$ cm⁻³) assuming an insignificant variation in length of the plasmoid along its passage. The values obtained by the two methods agree satisfactorily with each other. The increase in density with H_z is characterised by the following figures:

- (1) $H_z = 1$ kOe; $\rho = 2 \cdot 10^{15}$ cm⁻³; (2) $H_z = 3$ kOe; $\rho = 2 \cdot 10^{16}$ cm⁻³.

Azovskii, Akhmerov, Guzhovskii, Mazalov and Pistryak (UFTI) who experimented in conditions similar to the above but with blobs of smaller densities⁽²⁶⁾ were interested chiefly in the optical characteristics and the probe measurements. Hydrogen, or a mixture of 75% hydrogen and 25% helium, was admitted into the accelerator through a pulsed valve.

The broadening of the H_β spectral lines increased with increase in H_z . In a non-uniform field, where the blob is pinched, the H_β line contour resembles a Gaussian contour, and is obviously related to the Doppler effect. In a uniform field the line contour is diffuse and is mainly determined by the particle density. The electron temperature of the first blob was determined from the intensity ratio of the HeI(4921 Å) and HeI(4713Å) helium

* The diffusion of the field into a pinched blob, where T_{e1} may be higher, could not be measured by this method since the error of the measurement increases as the blob diameter decreases.

lines, its diameter from streak photographs. The charged particle density was determined from the half-widths of the H_{β} line.

A weak continuum is found in the radiation even for $H_z = 0$. In magnetic fields the continuous radiation is stronger by some order of magnitude, and is observed over the total visible spectrum.

Results of measurements of the radius R , the density n and the electron temperature

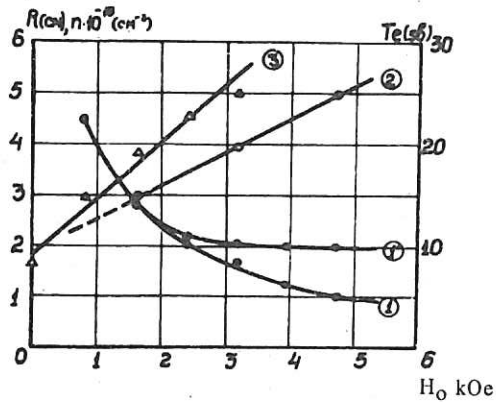


Fig. 23 (CLM-Trans 3)
Radius, density and electron temperature of plasma blob, plotted v magnetic field. 1 - radius of first blob. 1' - radius of second and following blobs. 2 - charged particle density. 3 - electron temperature

T_e for blobs in a magnetic field, are shown in Fig.23. The observed increase in the electron temperature from 10 to 25 eV occurs due to the conversion of the kinetic energy of the ions into electron energy. During compression the ions in the blob which, because of their inertia, penetrate fairly easily into the magnetic field, entrain along with them the electrons, thus increasing the energy of cyclic motion which due to collisions passes into thermal motion.

At the instant at which the blob enters the magnetic field, induced currents are set up in the blob creating their own H_z^* fields, whose value varies as a function of the initial (vacuum) field and the position of the blob. (Fig.24).

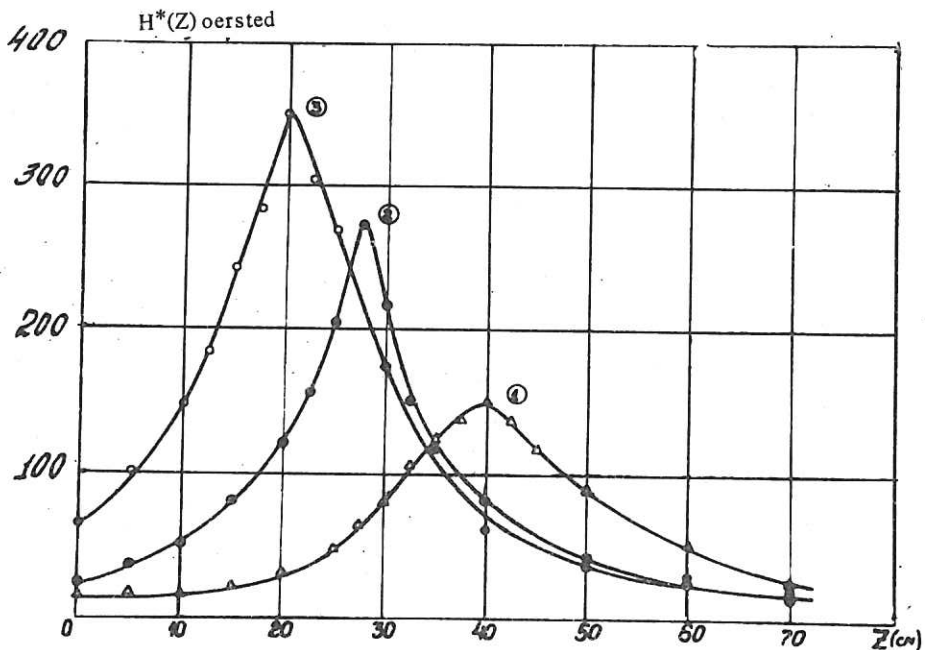


Fig. 24 (CLM-Trans 3)
Magnetic field of induced current (along the z-axis) plotted against position of blob in the magnetic field
(1) $B_0 = 300$ oersted (2) $B_0 = 1200$ oersted (3) $B_0 = 3300$ oersted

The induced H_z^* field increases as the blob enters the vacuum field, and reaches a maximum at the point z_{\max} . With an increasing radial compression H_z^* decreases rapidly despite the growth of $H_0(z)$. In the region where the induced current and the field increase (roughly proportionally to H_0) there is almost no magnetic field in the blob but the ratio $H_{(z_{\max})}^*/H_{0(z_{\max})}$ equals 0.85 at nearly all points over a wide range of H_{0z} . At this point, therefore, the magnetic field along the axis of the blob does not exceed 15% of H_{0z} .

It is interesting to note that in large fields, for $z > z_{\max}$ the velocity of the blob is almost doubled. It does not change in fields $H_0 \geq 300$ oersted. (sic) The reasons for this curious situation are not fully understood. The authors assume that it may be associated with the acceleration of the frontal part at the expense of the rest of the blob.

The possibility cannot be excluded that an important part is played by peculiarities of the blob structure in blobs from a given gun or by induced currents, leading to acceleration of separate particle groups. This effect was not, however, observed in Vasilyev's experiments where the condition for the formation of induction currents were also present.

Voitsenya, Gorbanyuk, Onishchenko, Safronov and Shkoda (UFTI) measured the polarising potentials set up in a blob during its passage through an axially-symmetric magnetic field.

The plasma from a conical source⁽²⁷⁾ was injected into a cylindrical glass tube of 6 cm in diameter placed in a uniform magnetic field. Before entering the field the plasma was collimated by three 2 cm apertures placed at 5 cm intervals. To screen the electric field of the source and to short-circuit the internal currents flowing in the plasma,

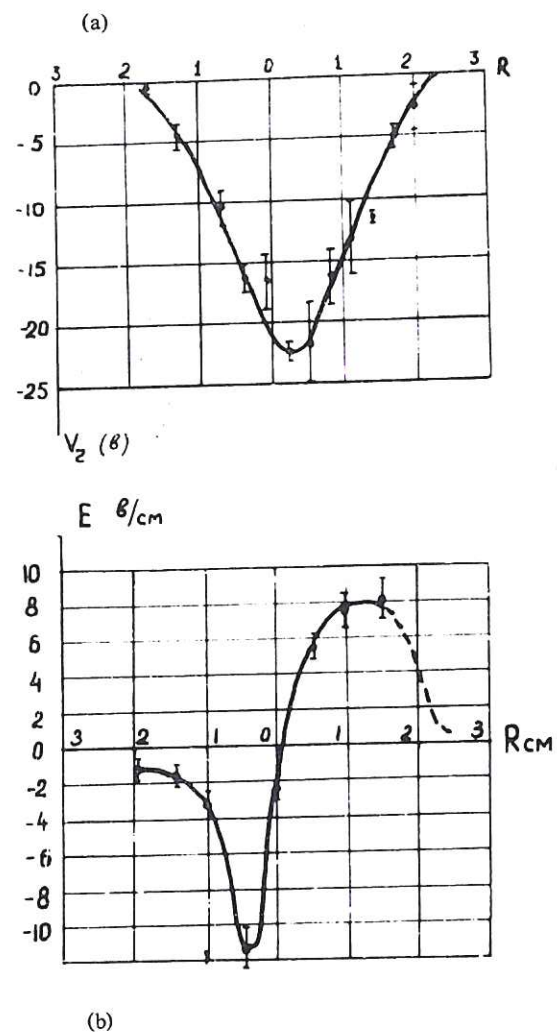


Fig. 25 (CLM-Trans 3)
 (a) Distribution of polarising potential over the vessel cross-section
 (b) Distribution of field gradient over the vessel cross-section

earthed grids were arranged in front of the apertured diaphragms.

The measuring probes were arranged at a distance of 50 cm from the source. The distribution of the polarising potentials 4 μ sec from the onset of the discharge (velocity of blob $1.2 \cdot 10^7$ cm/sec, $H_z = 700$ oersted) is shown in Fig.25(a).

The half-width of the potential curves immediately after the diaphragm is roughly equal to the diameter of the aperture, and then increases. The field strength (Fig.25(b)) at the maximum is 10 V/cm and in the direction toward the axis. The variation of the magnetic field gradient at the entry, and the eccentric arrangement of the chamber relative to the field axis did not affect the distribution of the polarising potential.

The authors believe that this can be attributed either to the different radii of the ions- and electron- orbits in the magnetic field of the solenoid, or to uncompensated space charge which, according to Post and Perkins⁽²⁸⁾ is invariably associated with a plasma blob in the magnetic field.

Kalmykov, Trubchaninov, Naboka (UFTI) observed rotation and instability of the plasma in the frontal part of the blob in the H_z field. The blob was produced by a coaxial gun and entered the solenoid (from which it was separated by 1.5 m) with a velocity of $8 \cdot 10^6$ cm/sec, and a mean particle density of $10^{13} - 10^{14}$ cm⁻³.

Because of its weak luminous intensity the blob had to be photographed with a plasmascop⁽²⁷⁾ which was introduced into the plasma. A series of photographs (Fig.26) shows first the compression of the blob on entering the magnetic field, then an increasing instability of the type of a spiral protuberance. When varying the direction

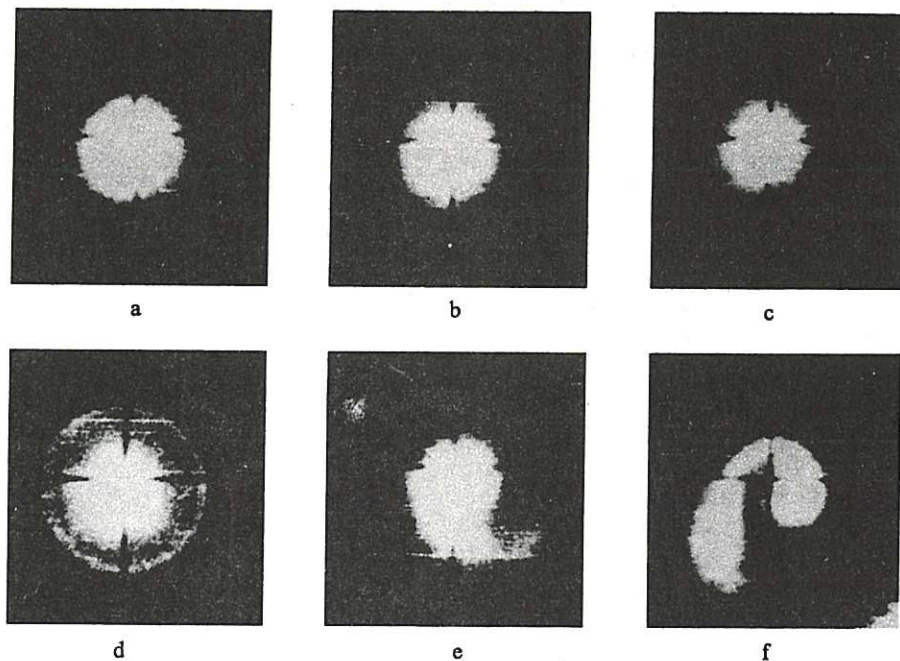


Fig. 26

(CLM- Trans 3)

Plasmagrams corresponding to the passage of a plasma blob through the H_z field (field of short solenoid)

- (a) $H_z = 600$ oersted; (b) $H_z = 750$ oersted; (c) $H_z = 1250$ oersted
- (d) $H_z = 1500$ oersted; (e) $H_z = 1600$ oersted (maximum field)
- (f) $H_z = 750$ oersted (after the maximum)

of the magnetic field the general picture of the motion of the plasma remains the same, but the direction of the spiral is reversed. A similar instability does not appear always but can be produced whenever a notch is made in the diaphragm. The plasma rotates with an angular frequency of around 250 kc/s.

The authors consider that the observed instability is of the Rayleigh-Taylor type, and that it develops due to the rotation of the plasma.

2. SEPARATION OF IMPURITIES BY A RAPIDLY INCREASING LONGITUDINAL MAGNETIC FIELD

As is widely known, the difference between the velocities of the plasma components referred to in earlier papers^(13,10,9) leads to separation of the highly ionized frontal portion of the blob, which moves with the highest velocity, from the tail where neutral and heavy particles are mainly concentrated. This phenomenon can be utilized for separating the second plasmoid from the first by means of a rapidly rising longitudinal magnetic field.

Vasilyev, Komelkov, Pergament, Tserevitinov, produced a rapidly rising field $T_f = 6.5$ μ sec by discharging a capacitor bank ($V_0 = 10$ kV; $C = 144$ μ F) into a single-loop coil of diameter 14 cm. At the instant the field reached its maximum of 25 kOe, a discharge gap short-circuiting the coil was switched on. The blob moved in a longitudinal magnetic field $H_z = 0.5$ kOe, which insulated it from the walls of the cylindrical glass tube 10 cm in dia. The separating field coil was situated at a distance of 120 cm from the end of the gun where the time separation or interval between the plasmoid fronts was 9.0 μ sec. The motion of the plasmoids was deduced from magnetic probe signals. As during the earlier investigations, the energy distribution in the plasmoids was calculated from the readings of thermal probes⁽³⁰⁾ placed 12 cm from the coil.

Photoelectric observation of the $H\beta$ and CII lines at 4267 \AA enables the instant to be determined at which the brightly luminous part of the blob enters a region situated 10 cm from the edge of the coil along the path of the blob.

Three conditions of motion of the plasmoids were investigated:

- (1) In the absence of a field (free motion).
- (2) With the field switched on, 4-5 μ sec before the arrival of the front blob (suppression).
- (3) With the separating field pulsed on 4.5 μ sec after the approach of the frontal part of the blob to the coil (separation).

Although the results obtained are of a provisional character, however, they demonstrate nonetheless different characteristics of the blobs under these three conditions. Oscillograms of the separating magnetic field, and of current and gun potential, the diamagnetic and photoelectric signals for all three sets of conditions, are reproduced in Fig.27. They

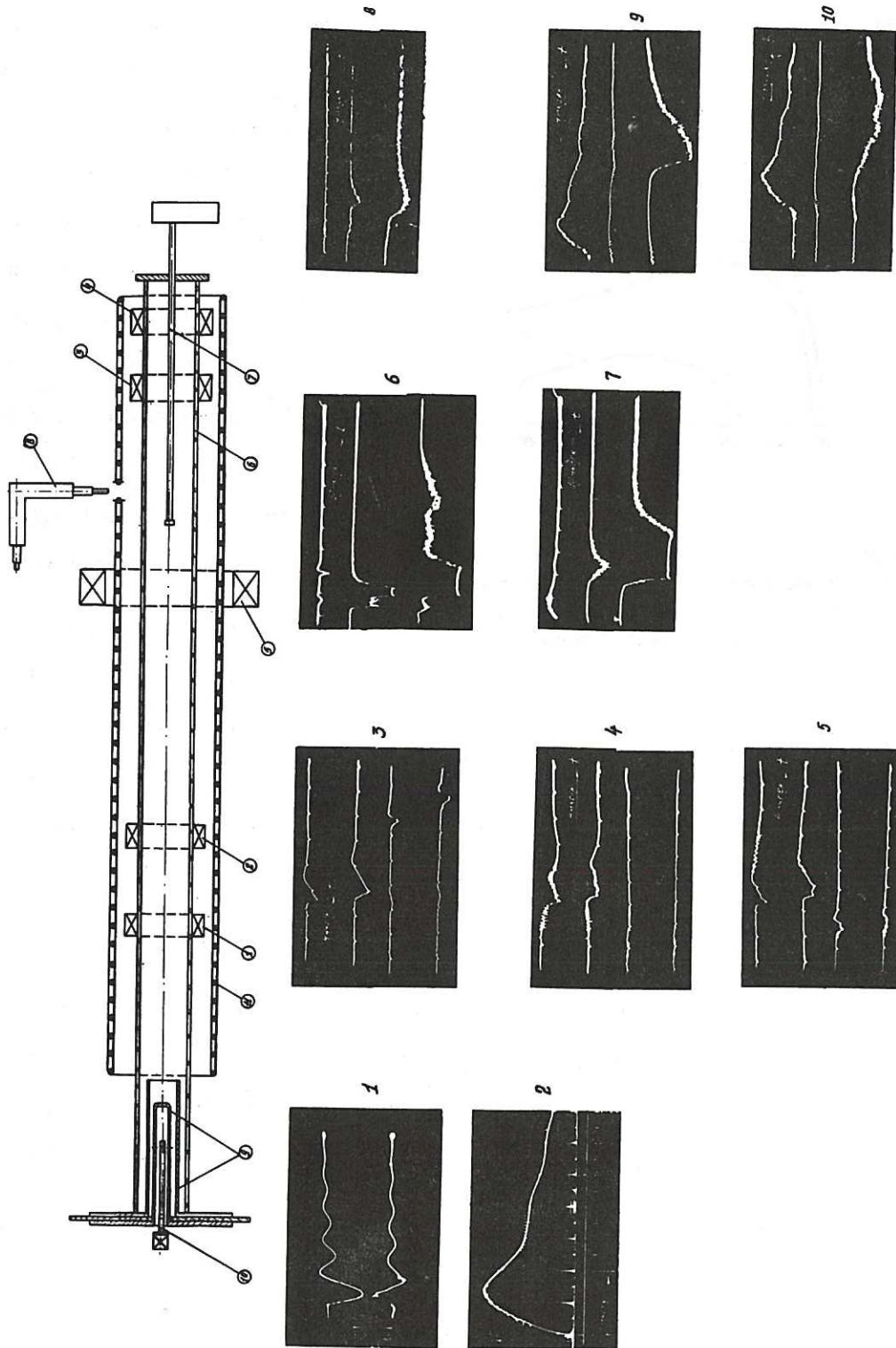


Fig. 27

(CLM-Trons3)
 Apparatus and oscillograms of signals for separation of plasmoids by rapidly rising magnetic field
 1, 2, 3, 4 - diamagnetic loops; 5 - separating coil; 6 - glass tube, 100 mm dia; 7 - movable thermal probe; 8 - monochromator; 9 - gun electrodes; 10 - electrodynamic gas valve; 11 - guiding longitudinal field coil.
 Oscillograms:
 1 - gun current and potential; 2 - current in separating field coil; 3 - signals of coils 1, 2, 3, 4 (top to bottom) during motion of plasmoid in longitudinal field, without separating field; 4 - separating coil switched on before arrival of front blob; 5 - separating coil switched on; 6 - (omitted on original); 7 - signals (top to bottom); separating current, CII intensity, H β intensity (at tube centre); 8 - signals (top to bottom); time markers; CII intensity, H β intensity (edge of tube)
 9 - as 8, 'suppression'; 10 - as 8, 'separation'

show that in the region of coils 3 and 4 the time interval between the plasmoids in condition one is 12 and 16 μsec respectively. In the 'suppression' conditions signals from the diamagnetic probes of the same coils, associated with the arrival of the rapidly moving ionized portion of blob, have completely vanished.

The $H\beta$ and CII lines appear in the 'separation' conditions at the same instant at which the second plasmoid usually arrives in the 'free motion' conditions.

This means that the ionized blob, arriving at the separating field of 20 kOe, is reflected by the barrier, whilst the blob containing the large proportion of neutral particles will pass through it (12 kOe on arrival of the second blob).

In addition to the light emission the thermal probe (Fig.28) also registers, in the central region, the arrival of the

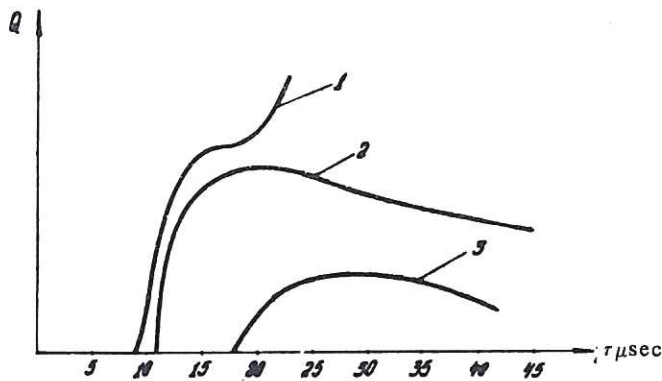


Fig. 28 (CLM-Trans 3)
Thermal probe signals. 1 - without separating field;
2 - 'separation'; 3 - 'suppression' (field switched on
before arrival of blob)

second blob. The first blob is not registered by this probe although, as was shown earlier⁽⁹⁾, its energy is fairly large. The second blob remains compressed behind the coil, as indicated by the considerable loss of intensity of the $H\beta$ and CII lines near the tube walls compared with the conditions of 'free motion'.

In the 'separation conditions' the thermal probe only registers the first plasmoid. For 50 μsec

no new blobs arrive at the probe although the $H\beta$ line appears near the walls and in the centre. Most probably, some of the neutrals still penetrate through the field, although their energy is considerably smaller than during free motion of the blob.

3. INTERACTION OF PLASMA BLOBS WITH A TRANSVERSE MAGNETIC FIELD

Earlier investigations^(31,32) of the interaction of plasma blobs with a transverse magnetic field showed that only one part of the blob passes through the field, the other part being trapped by the latter and propagating in both directions along the magnetic field lines. This velocity of propagation is greater than the initial velocity of the plasma.

Demidenko, Padalko, Safronov and Sinelnikov⁽³³⁾ studied the motion and configuration of

a plasma injected into a transverse magnetic field by plasmascopes^(39,34) magnetic and electric probes and Thomson mass spectrograph.

The experimental arrangement is shown in Fig.29. The blob was produced by the perspex conical electrode induction source described in reference 17.

To permit adequate localisation of the beam and to facilitate observation of its behaviour, a diaphragm with 10 mm aperture was placed at the point of entry into the magnetic field.

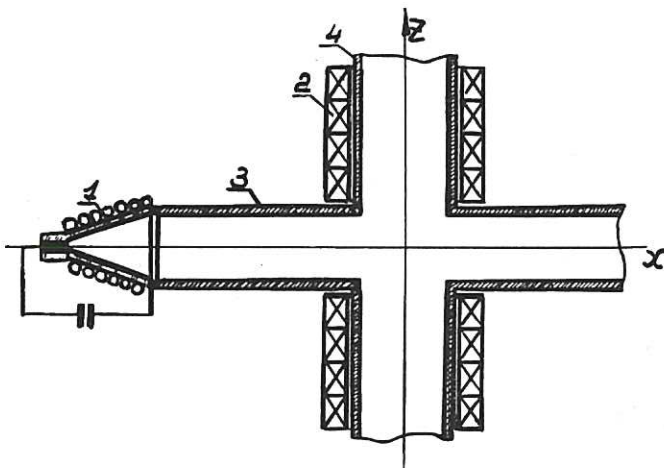


Fig. 29
Experimental apparatus. 1 - electrode-induction source (of plasma blobs); 2 - solenoid; 3 - copper plasma guide; 4 - copper vessel

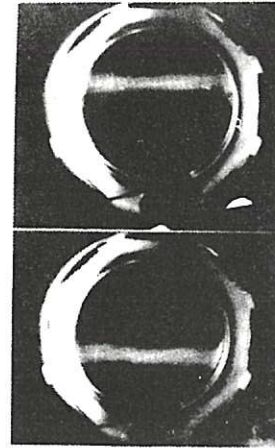


Fig. 30
Plasmagrams obtained in xy plane, $z = 2$ cm, with opposing magnetic field directions, $H = 270$ oersted. Injection from left. Aperture in plasma guide 1 cm

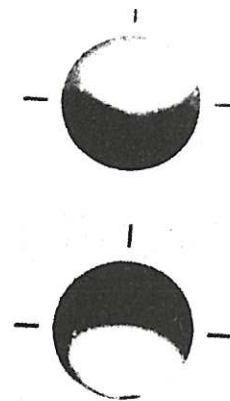


Fig. 31 (CLM-Trans 3)
Plasmagrams obtained in zy plane for $x = 5$ cm (limit of vessel) with opposing directions of magnetic field, $H = 270$ oersted. Aperture in plasma guide 1 cm

Fig.30 is a (plasmascopes) photograph of the plasma in a plane perpendicular to the magnetic field; the picture remains virtually unaffected by the position of the plasmascopes relative to the point of injection.

Fig.31 is a similar picture of the plasma in a plane near the wall opposite to the point of entry of the plasma. It follows from both pictures that the plasma blob is displaced upward or downward with respect to the axis depending on the direction of the magnetic field. This displacement can be explained by longitudinal polarisation of the blob

as it passes through the magnetic gradient. The longitudinal polarisation vector is always in the direction opposite to the motion of the blob, and the blob on entering the field is consequently subject to a drift in the crossed fields in a direction perpendicular to that of the injection. In a uniform magnetic field this drift vanishes, the polarisation becoming perpendicular to the velocity of propagation. To verify that the plasma in fact diffuses along the lines of force a diaphragm with five vertical slots was placed perpendicular to the magnetic field; after this diaphragm was arranged the plasmascope which could be moved away from the diaphragm by 30 cm without going beyond the limits of the magnetic field. As Fig.32 shows, the plasma fluxes follow the magnetic field lines fairly closely.

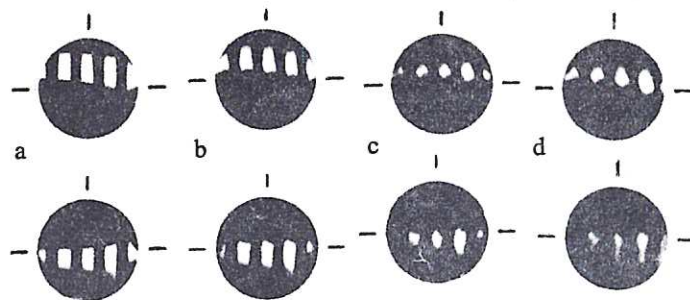


Fig. 32
Plasmagrams showing trapping by the magnetic field of a plasma split up by slots in a diaphragm placed into the solenoid at a distance $z = 8$ cm. Width of the slots 0.8 cm. Diameter of plasmascope 7 cm. Injection from the right. a (1 cm), b (10 cm), c (20 cm), d (30 cm) mark the distances by which the plasmascope is moved away from the slotted diaphragm, $H = +270$ oersted

Using magnetic probes moving along the X-axis, the variation was investigated of the

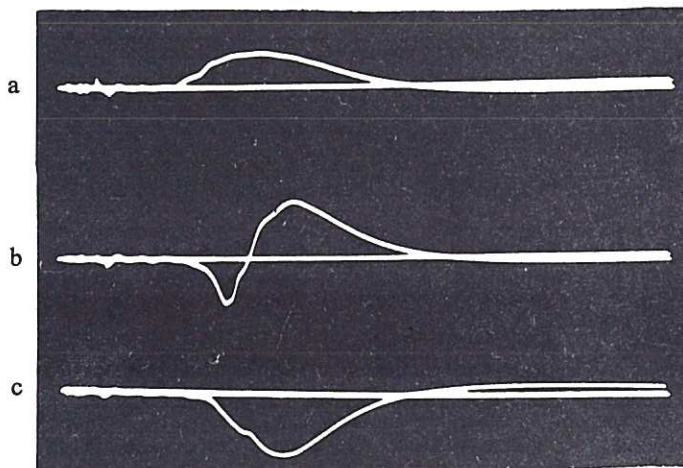


Fig. 33 (CLM-Trans 3)
Integrated magnetic probe signals
a) $x = -15$ cm; b) $x = -1$ cm; c) $x = +11$ cm

magnetic field during the propagation of the blob in the transverse field. As the oscillograms in Fig.33 show, there is some displacement of the magnetic field at the entry. In the region of the axis, the probe registers first a compression or intensification of the field; then, immersed into the arriving plasma, it registers attenuation of the magnetic field; lastly, beyond the vessel, at the exit,

an intensification of the vacuum magnetic fields is observed which may be treated as an extension (or 'carrying out beyond the walls') of the magnetic field by the plasma.

From a comparison of the absolute values of the induced magnetic field and the vacuum

field it is apparent that the former barely attains 2% of the value of the latter at the point in question. This indicates fairly deep penetration of the magnetic field into the plasma during the passage of the blob.

A considerable decrease in the density of the plasma (several orders) leading to a corresponding attenuation of the induced magnetic fields, did not, however, lead to a noticeably changed behaviour of the blob. The authors therefore drew the conclusion that obviously the behaviour of the plasma is not related to the presence of the induced fields in the blob.

The Thomson mass spectrograph⁽³⁵⁾ was used to measure the mass composition of the plasma propagating across, and parallel to, the magnetic field, and also without the field.

Whilst moving across the magnetic field, the plasma contains less hydrogen and multiply-charged impurities. Thus, after passing through a field of about 700 gauss, only 5% of the initial hydrogen ions remain in the blob. Along the lines of force propagates a plasma consisting of H^+ and C^+ . As the field increases the hydrogen content increases, reaching 60%, whilst the hydrogen content in the initial plasma was only 11%.

Electric probe measurements showed that the mean velocity of propagation of the plasma parallel to the magnetic field increases as the field increases, and that at maximum fields it may be double or treble the mean transverse velocity.

This problem was also studied by Demidenko, Padalko, Safronov and Sinelnikov by means of a time-of-flight mass analyser⁽³⁶⁾ giving the mass- and energy spectra of the ions. They observed that the generation of the plasma blob takes place during a very short interval of time, at the start of the first half period of the discharge current of the gun. The pulse widths on the mass spectrogram are consequently small. This enables the energies of the ions to be determined from the length and the time-of-flight across the distance between the plasma source and the detector.

Because of the difficulties encountered in registering ions of small energy the authors only investigated ion distribution for energies up to 80 eV as a function of the magnetic field.

Fig.34 shows the distribution of the H^+ , C^+ and Al^+ ions passing through the transverse magnetic field. As the latter is increased the energy of the ions decreases. Thus, for a field of 25 oersted the energy distribution of the protons is limited to 600 eV, at 150 oersted this energy drops to 200 eV. A similar picture is presented by the distribution of the C^+ and Al^+ ions, although for these the dependence of the limiting energy on the field is much weaker, and intervenes at higher fields.

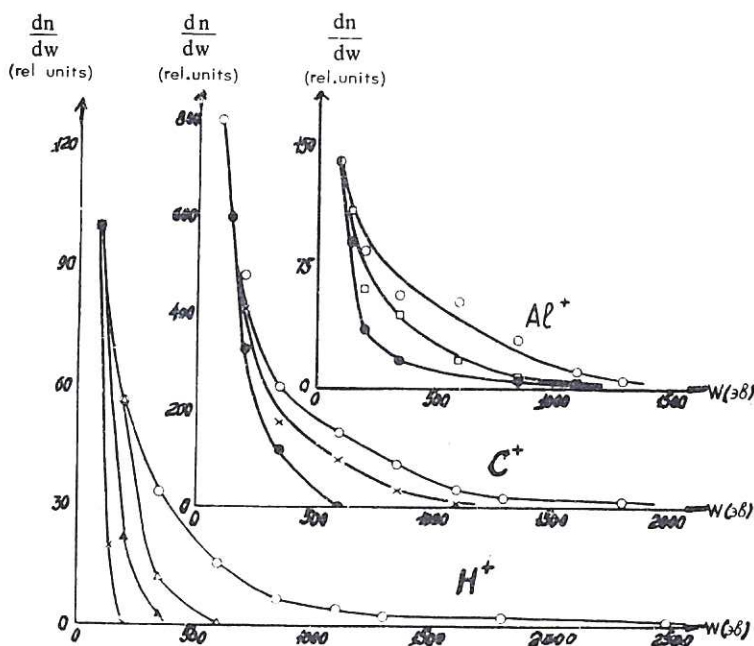


Fig. 34 (CLM-Trans 3)
 Energy spectra of H^+ , C^+ and Al^+ ions in a plasma direct from the source, and in a plasma passed through transverse magnetic fields: O - 0 gauss; Δ - 25 gauss; \blacktriangle - 75 gauss; X - 150 gauss; \square - 300 gauss, \blacksquare - 500 gauss. Different scales along the ordinates for the different ions and magnetic field strengths.

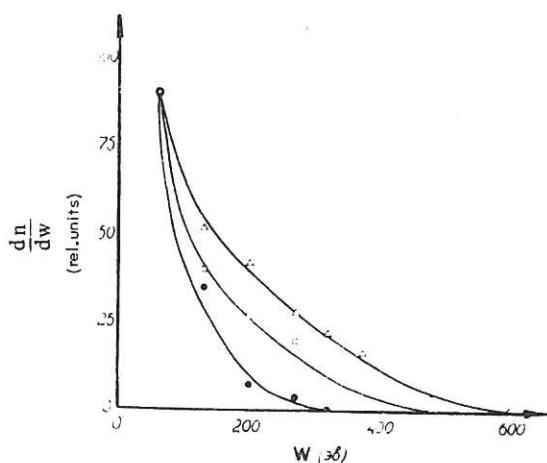


Fig. 35 (CLM-Trans 3)
 Energy spectra of H^+ in a plasma moving in the direction of the magnetic field. Δ - $H = 500$ gauss, \square - $H = 300$ gauss, \bullet - $H = 25$ gauss. Different scales along the ordinates for the different magnetic field strengths

The energy of the ions following the direction of the magnetic field, is distributed in the opposite way. The longitudinal energy of the hydrogen ions increases as the magnetic field is increased. Fig. 35 shows that for $H = 25$ oersted the limiting energy is 300 eV, for $H = 500$ oersted it rises to 600 eV, in conjunction with a simultaneous increase in the absolute quantity of ions with intermediate energies.

From the mass-spectrograms of the plasma moving parallel and perpendicularly to the magnetic field it follows that the

pulse widths registered for ions of given energies remain the same as without the magnetic field.

Moreover, (with an accuracy of 10%) the transit time of the plasma corresponds to the recorded ion energy. All this points to the existence of a very rapid collisionless process transforming the transverse ion velocity into a longitudinal velocity.

To analyse this process Demidenko, Lomino, Padalka, Safranov and Sinelnikov investigated the electric polarisation set up during the motion of the plasma across the magnetic field, and its effect on the motion of the plasma parallel to the field.

The length of the solenoid was increased to 150 cm in both directions from the point of entry of the plasma, and the magnetic field could be varied from 0 to 1600 oersted; the diameter of the vessel with the longitudinal magnetic field was also slightly increased. All the remaining parameters were left unchanged.

Fig.36 summarises the results of measurements of the polarising field E_y (perpendicular to the direction of v_0 of the plasma and the magnetic field of the solenoid) as a function of the probe position along the z-axis. It is seen that the plasma, propagating along the lines of force, is polarised up to a distance of nearly 100 cm. A two-fold increase of the magnetic field leads to a roughly twofold increase in the polarisation.

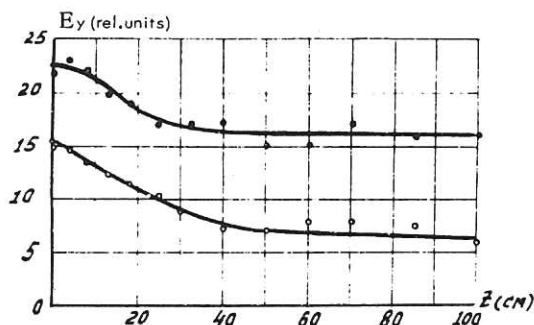


Fig. 36 (CLM-Trans 3)
Dependence of polarising field on probe position along the solenoid axis. The point of injection of the plasma in the magnetic field corresponds to $z = 0$

- $H = 1.6 \cdot 10^5$ amp turns per metre
- $H = 8 \cdot 10^4$ amp turns per metre

It was known from⁽³⁷⁾ that the short-circuiting of the polarising field of the plasma moving through the transverse magnetic field, slows down the plasma flux.

Demidenko, et al assumed that since the polarisation is maintained during the motion of the plasma along the whole solenoid, a metal plate will short-circuit the electric polarising field not only when placed at the point of injection, but also when placed at a point relatively remote from the point of injection along the solenoid. In this case short-circuiting must be effected by the plasma trapped by the magnetic field and propagating parallel to the lines of force (in the direction opposite to that of the plasmascop).

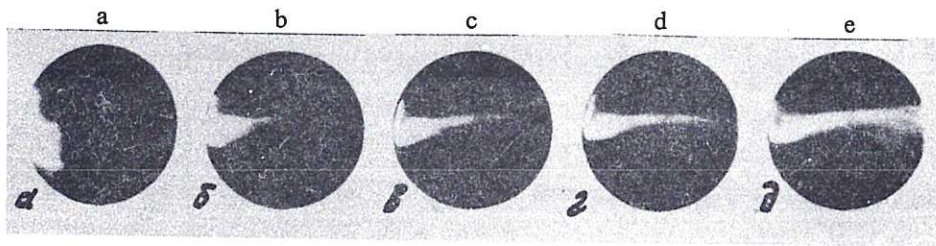


Fig. 37
 Series of plasmagrams, obtained for different distances between the short-circuiting plate and the point of injection of the plasma in the solenoid ($z = 0$); injection from the left. a) $z = 0$ cm; b) $z = -2$ cm; c) $z = -4$ cm; d) $z = -7$ cm; e) $z = -40$ cm; $H = 400$ oersted

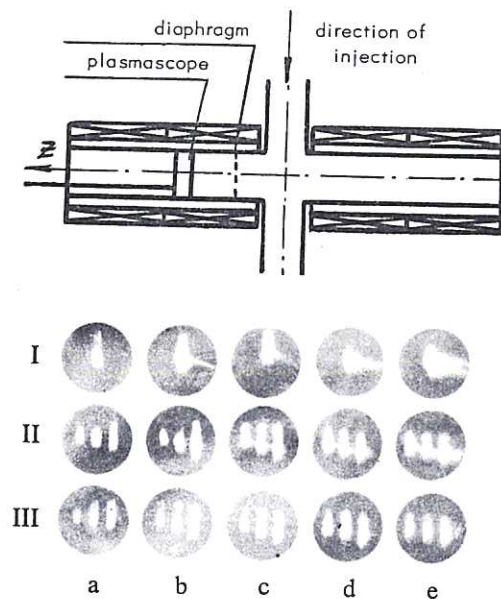


Fig. 38 (CLM-Trans 3)
 Experimental apparatus and plasmagrams obtained for different distances between slotted diaphragm and point of injection, and different distances between plasmascope and diaphragm. Diaphragm - injection: I = 8.5 cm; II = 12 cm; III = 25 cm. Plasmascope - diaphragm: a = 0 cm; b = 15 cm; c = 40 cm; d = 65 cm; e = 90 cm. $H = 800$ oersted

From the plasmagrams in Fig.37 it is apparent that whilst the plasma continues to move across the magnetic field i.e. during the existence of the polarising field E_y , the plasma is ejected parallel to the magnetic field. As soon as the plasma strikes the metallic short-circuiting plate, its ejection stops. Plasma which had started to move along the lines of force up to the instant of short-circuiting, continues its motion unaffected.

The plasma with polarisation E_y must experience a drift across the magnetic field. This could in fact be observed during the following experiments. The (insulating) slotted diaphragms split up the plasma trapped by the longitudinal magnetic field, into a number of flat beams or bands in which the polarisation was maintained. It was found that as the plasmascope was moved progressively further away from the diaphragm, an initially narrow but gradually broadening spread (drift) of the plasma from the centre of the strip towards the walls was observed. This drift becomes less evident as the diaphragm is moved further away from the point of injection (Fig.38).

One explanation would obviously seem to be that as the diaphragm is moved further away to regions of smaller polarisation, the drift in the direction toward the wall is slowed down.

The results of these experiments suggest that one reason for the diffusion of the plasma along the line of force might well be the electric field of the surface charges set up during the polarisation of the plasma. The motion of the charges in this electric field will most probably be along the lines of force of the magnetic field. Following from this hypothesis, the selective propagation of the fast particles along the force lines becomes understandable, since the primary part in producing the polarising potentials is played by the particles with the highest energies. Because of their large Larmor radius in the collisionless plasma they are capable of passing beyond its boundary, where they then find themselves in the space charge field by which they are compelled to propagate parallel to the magnetic field. Naturally the first to start in this direction will be the hydrogen ions and, their energy increasing in the electric field, they will reduce the electrostatic potential of the polarising layer; this in turn invites into the layer a fresh stream of particles whose energies will be smaller than those of the first batch but still sufficiently large to maintain the polarising potential of the charged particle layer at a sufficiently high level, and this will continue almost down to ions with low energies. This picture might explain the energy distribution of the ions measured parallel to the field, and the disappearance of high energy ions in a plasma passing across the field.

The density of the trapped plasma was measured to be of the order of 10^{11} at a distance farther than 50 cm from the point of injection, for a density of the injected plasma of the order of 10^{13} .

The described properties of a plasma trapped by a magnetic field and propagating along the lines of force of this field, appear very attractive from the point of view of filling magnetic traps, especially of the 'Stellarator' type.

CONCLUSIONS

1. Pulsed plasma guns are hitherto the only sources of high density plasma. The plasma blobs generated by these sources have frontal velocities in excess of 10^8 cm/sec. They carry, however, a multi-component plasma with a high content of impurities originating from the insulators and electrodes. It is essentially the presence of the latter, and of the neutral particles, which renders the plasma obtained from such guns unsuitable for use in certain thermonuclear experiments. Only the frontal part of the blob is ionized and can be used for studying the interaction of the blobs with the magnetic field.

The following methods of purifying the plasma are proposed and have been developed:

- (a) the choice of conditions in which the quantity of these impurities is kept to a minimum. Such conditions are not always acceptable, as they lead to a reduced velocity of the blob, and to an increased quantity of neutrals in the blob;
- (b) damping of the circuit with linear and non-linear resistances so as to achieve aperiodic discharge conditions;
- (c) clamping of the external gun circuit at the end of the first half period, at the maximum of the current, or at the moment at which large quantities of impurities enter the discharge;
- (d) separation of the un-ionized part of the blob from the ionized portion, and of the fast particles from the slow ones during some section along the path of the blob; separation of the ionized part of the blob from the un-ionized portion of a rapidly increasing longitudinal magnetic field. This is conveniently combined with the trapping of the blob (see (e));
- (e) trapping of the blob in toroidal and transverse magnetic fields or in cusp fields;
- (f) filtering out the neutral particles in a spatially periodic cusped magnetic field, or in large diameter chambers with longitudinal magnetic field.

The accumulated experimental evidence justifies the assumption that the removal of the neutral and slow particles from the blobs is possible.

2. In cylindrical coaxial guns one has two different operating conditions. One in which the plasma moves between the electrodes, and the 'fountain pinch' in which the plasma is carried with the current beyond the ends of the electrodes. From the point of view of obtaining high velocity frontal plasmoids the most effective is the 'fountain pinch' which is realized in its purest form in the Bostick type gun (end type gun).

The current plasmoids generated by guns of the various types, can persist for considerable periods of time both without a magnetic field and in a longitudinal magnetic field, a fact which must be borne in mind when studying the interaction between blobs and fields with various configurations.

3. The optimum operating conditions of a gun from the point of view of obtaining a pure plasma are related to the initial distribution of the gas in the working volume, which to some degree determines the so-called channel structure.

This structure, which contributes to the development of local increases in current density (separate channels) leads to an intense release of impurities into the discharge. The formation of the plasma piston is improved and the channel structure reduced when the gas is pre-ionized. In this connection the so-called cascade guns are of interest in which in addition the plasma is also accelerated.

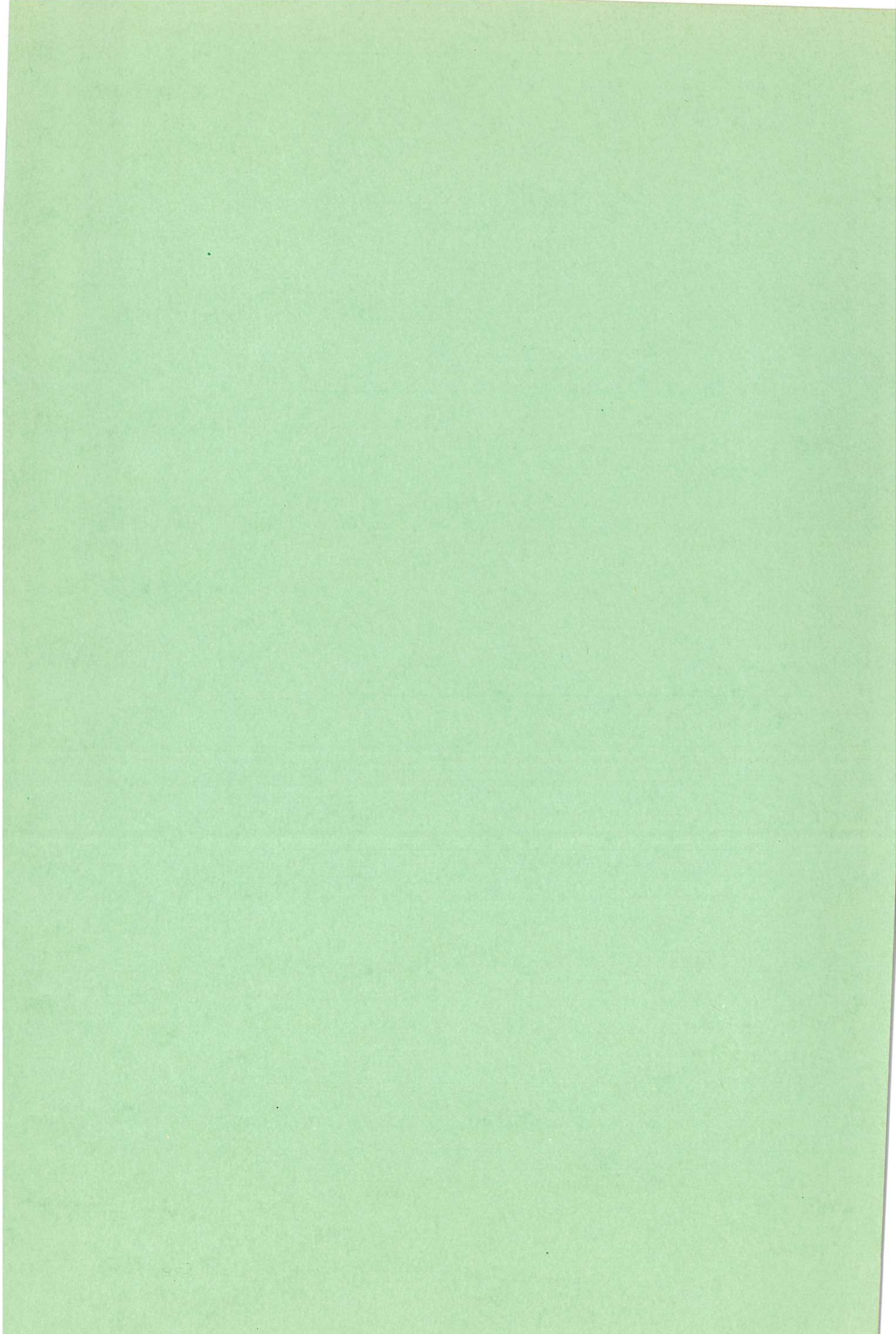
4. The nature of the fast particles, and the mechanism of formation of the so-called 'boosted' blobs, which move at velocities exceeding that of the current layer, is not yet understood. The above-mentioned structure of the magnetic fields in blobs carrying currents, points to the possibility of the formation of accelerating electric fields in these blobs.

5. The experimental results emphasize that the snowplough model is not suitable to describe the acceleration processes taking place in guns. Further investigations are necessary into the interaction between the current layer and the neutral gas, and efforts must be made to formulate mathematical relationships which would take into account the processes taking place in the gas and at the electrodes more extensively than hitherto.

REFERENCES

1. ARTSIMOVICH, L.A., LUK'YANOV, S.YU., PODGORNII, I.M. and CHUVATIN, S.A. Zhurnal Eksperimentalnoi i Teoreticheskoi Fiziki, 33, 1 (7) 1957, p.3.
2. MARSHALL, J. Physics of Fluids, 3, 134 (1960)
3. KOMELKOV, V.S., Zhurnal Eksperimentalnoi i Teoreticheskoi Fiziki, 35, 1, 6 (1958)
4. KOMELKOV, V.S., SKVORTSOV, YU.V., TSEREVITINOV, S.S. Proceedings of the 2nd International Conference on Peaceful Uses of Atomic Energy. Atomizdat 1959.
5. VASILEV, V.I., KOMELKOV, V.S., SKVORTSOV, YU.V., and TSEREVITINOV, S.S. Zhurnal Tekhnicheskoi Fiziki, 30, 756 (1960).
6. KOMELKOV, V.S., SKVORTSOV, YU.V., TERESHCHENKO, V.N. and TSEREVITINOV, S.S. Proceedings of the 5th International Congress on Ionization Phenomena in Gases. Minsk, 1961.
7. BOSTICK, W.H. Progress in Nuclear Energy. Series XI, vol.2, (1963) Pergamon Press.
8. BARANOV, V.YU., and MUSIN, A.K., Radiotekhnika i Elektronika, 9, 281-290, (1964).
9. ARETOV, G.N., VASILEV, V.I., KOMELKOV, V.S., PERGAMENT, M.I. and TSEREVITINOV, S.S. Proceedings of 6th International Congress on Ionization Phenomena in Gases, Paris, July, 1963.
10. KALMYKOV, A.A., TIMOFEEV, A.D., PANKRATEV, YU.I., TERESHIN, V.I., TRUBCHANINOV, S.A., NABOKA, V.A., NOZDRACHEV, M.G. and SAFRONOV, B.G. Proceedings of the 6th International Congress on Ionization Phenomena in Gases, Paris, July, 1963.
11. KALMYKOV, A.A., TIMOFEEV, A.D., MARININ, V.G., and SIVAGIN, F.V. Ukrain. Fiz. Zh. (1964).
12. KOMELKOV, V.S. Proceedings of the 2nd International Conference on the Peaceful Uses of Atomic Energy, Geneva, 1958.
13. DEMICHEV, V.F., MATYUKHIN, V.D. Doklady Akademii Nauk, SSSR, 156, 279, 2, (1963)
14. Optical Pyrometry of Plasmas. (Collection of Articles, published 1962).
15. KOMELKOV, V.S., SKVORTSOV, YU.V., TSEREVITINOV, S.S. and VASILEV, V.I. Proceedings of the 4th International Congress on Ionization in Gases, Uppsalam, Sweden, 1959.
16. OSHER, J.E., HAGERMAN, D.E. Review of Scientific Instruments, vol.34, no.1, p.56, (1963).
17. AZOVSKII, YU.S., GUZHOVSKII, I.T., SAFRONOV, B.G. and CHURAEV, V.A. Zhurnal Tekhnicheskoi Fiziki, 32, 1050 (1962).
18. BORZUNOV, N.A., ORLINSKII, D.V. and OSOVETS, S.M. Zhurnal Eksperimentalnoi i Teoreticheskoi Fiziki, 36, 3, (1959)

19. SCOTT, F.R. and VOORHIES, H.G. Physics of Fluids, 4, no.5, (1961)
SCOTT, F.R. and ELDRIDGE, O.C. Physics of Fluids, 4, no.12, (1961)
20. COESGEN, F.H., CUMMINS, W.F., SHERMAN, A.E. Physics of Fluids, 2, 350, (1959)
21. EHELS, RABI and others. Review of Scientific Instruments, 29, 614, (1958).
22. SINELNIKOV, K.D., AZOVSKII, YU.S., GUZHOVSKII, I.T., PANCHENKO, V.E. and SAFRONOV, V.G. Zhurnal Tekhnicheskoi Fiziki, 33, 10 (1963) and also 2nd Paper in Conference on Plasma Physics Fiz. Tekh. Inst. Akad. Nauk. Ukrain. SSR. Izvest. Akad. Nauk. Ukrain. SSR. Kiev, 1963.
23. DEMICHEV, V.F., STRUNNIKOV, V.M. Doklady Akademii Nauk, SSSR, 150, 3, (1963)
24. ARETOV, G.N., VASILEV, V.I., KOMELKOV, V.S., PERGAMENT, M.I. and TSEREVITINOV, S.S. Paper at the Conference on Controlled Thermonuclear Reactions, Salzburg, 1961.
25. FILIPPOVA, T.I., FILIPPOV, N.V. and VINGRADOV, V. Nuclear Fusion, 195 - 197, (1961)
26. AZOVSKII, YU.S., GUZHOVSKII, I.T., SAFRONOV, B.G. Zhurnal Tekhnicheskoi Fiziki, (1964)
27. AZOVSKII, YU.S., GUZHOVSKII, I.T., et al. Inzhenerno - Fizicheskii Zhurnal, 9, 57, (1963).
28. PERKINS, W.A. and POST, R.F. Physics of Fluids, 6, 11, 1537, (1963)
29. ELIZAROV, L.I. and ZHARINOV, A.V., Nuclear Fusion, p.2, 699 (1962)
30. PROKHOROV, YU.G., Doklady Akademii Nauk, SSSR, 134, 5, (1960)
31. HARRIS, E.G., THENS, R.B. and BOSTICK, W.H. Physical Review, 105, 47 (1957)
32. SAFRONOV, B.G., GONCHARENKO, V.P. and GONCHARENKO, D.K. Physics of Plasmas and Problems of Controlled Thermonuclear Fusion, 1, A.N. Ukrain, SSR Kiev, 1962.
33. DEMIDENKO, I.I., PADALKA, V.G., SAFRONOV, B.G. and SINELNIKOV, K.D., Zhurnal Tekhnicheskoi Fiziki, 34, 7, 43, (1964)
34. SINELNIKOV, K.D., SAFRONOV, B.G., PADALKA, B.G. and DEMIDENKO, I.I. Zhurnal Tekhnicheskoi Fiziki, 33, 1055 (1963).
35. KONOVALOV, I.I., KRUPNIK, L.I., ONISHCHENKO, I.N., and SHULIKA, N.G. Plasma Diagnostics, Gosatomizdat, 1963.
36. KALMYKOV, A.A., TIMOFEEV, A.D., PANKRATEV, YU.I., TERESHIN, V.I., VERESHCHAGIN, V.L. and ZLATOPOLSKII, L.A. Pribory i Tekhnika Eksperimenta, 142, 5, (1963)
37. BAKER, D.A. and HAMMEL, J.E. Physical Review Letter, 8, 157, (1962)



Available from
HER MAJESTY'S STATIONERY OFFICE
York House, Kingsway, London W.C. 2
423 Oxford Street, London W. 1
13a Castle Street, Edinburgh 2
109 St. Mary Street, Cardiff
39 King Street, Manchester 2
50 Fairfax Street, Bristol 1
35 Smallbrook, Ringway, Birmingham 5
80 Chichester Street, Belfast
or through any bookseller.

Printed in England